CHAPTER

The Elastic Stress Field around a Crack Tip

3

Brittle fracture in a solid in the form of crack growth is governed by the stress field around the crack tip and by parameters that describe the resistance of the material to crack growth. Thus, the analysis of stresses near the crack tip constitutes an essential part of fracture mechanics. For brittle materials exhibiting linear elastic behavior, methods of elasticity are used to obtain stresses and displacements in cracked bodies. These methods include analytical ones, such as the complex potential function method and the integral transform method, and numerical ones, such as the finite element method. In this chapter, the complex potential function method is introduced and used to analyze the stresses and displacements around crack tips. The characteristics of the near-tip asymptotic stress and displacement fields and the crack growth criterion based on the crack tip field are discussed.

3.1 BASIC MODES OF FRACTURE AND STRESS INTENSITY FACTOR

A crack in a solid consists of disjoined upper and lower faces. The joint of the two crack faces forms the crack front. The two crack faces are usually assumed to lie in the same surface before deformation. When the cracked body is subjected to external loads (remotely or at the crack surfaces), the two crack faces move with respect to each other and these movements may be described by the differences in displacements u_x, u_y, and u_z between the upper and lower crack surfaces, where (x, y, z) is a local Cartesian coordinate system centered at the crack front with the x-axis perpendicular to the crack front, the y-axis perpendicular to the crack plane, and the z-axis along the crack front.

There are three independent movements corresponding to three fundamental fracture modes as pointed out by Irwin [3-1], which are schematically illustrated in Figure 3.1. These basic fracture modes are usually called Mode I, Mode II, and Mode III, respectively, and any fracture mode in a cracked body may be described by one of the three basic modes, or their combinations (see their descriptions on the next page).

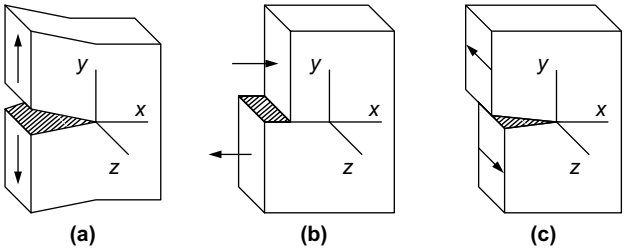

FIGURE 3.1

Schematic of the basic fracture modes: (a) Mode I (opening), (b) Mode II (sliding), (c) Mode III (tearing).

1. *Mode I (Opening Mode)*: The two crack surfaces experience a jump only in u_y, that is, they move away symmetrically with respect to the undeformed crack plane (xz-plane).
2. *Mode II (Sliding Mode)*: The two crack surfaces experience a jump only in u_x, that is, they slide against each other along directions perpendicular to the crack front but in the same undeformed plane.
3. *Mode III (Tearing Mode)*: The two crack surfaces experience a jump only in u_z, that is, they tear over each other in the directions parallel to the crack front but in the same undeformed plane.

The three basic modes of crack deformation can be more precisely defined by the associated stresses ahead of the crack front, which may be considered as the crack tip in two-dimensional problems. It will be seen in the following sections that the near-tip stresses in the crack plane (xz-plane) for these three modes can be expressed as ($y = 0,\ x \to 0^+$)

$$\begin{aligned}
\sigma_{yy} &= \frac{K_I}{\sqrt{2\pi x}} + O(\sqrt{x}), \quad \sigma_{xy} = \sigma_{yz} = 0 \\
\sigma_{xy} &= \frac{K_{II}}{\sqrt{2\pi x}} + O(\sqrt{x}), \quad \sigma_{yy} = \sigma_{yz} = 0 \\
\sigma_{yz} &= \frac{K_{III}}{\sqrt{2\pi x}} + O(\sqrt{x}), \quad \sigma_{yy} = \sigma_{xy} = 0
\end{aligned} \tag{3.1}$$

respectively, where the three parameters K_I, K_{II}, and K_{III} are named stress intensity factors corresponding to the opening, sliding, and tearing (anti-plane shearing) modes of fracture, respectively.

These expressions show that the stresses have an inverse square root singularity at the crack tip and the stress intensity factors K_I, K_{II}, and K_{III} measure the intensities of the singular stress fields of opening, in-plane shearing, and anti-plane shearing, respectively. The stress intensity factor is a new concept in mechanics of solids and

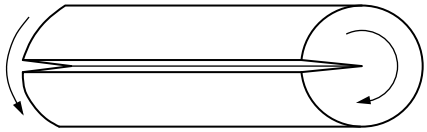

FIGURE 3.2

Mode III deformation in a cracked cylinder under torsion.

plays an essential role in the study of fracture strength of cracked solids. Various methods for determining stress intensity factors, including analytical, numerical, and experimental approaches, have been developed in the past few decades.

It is important to note that, except for Mode I deformation shown in Figure 3.1(a), the loading and specimen geometries shown in Figures 3.1(b) and (c) cannot be used to produce pure Mode II and Mode III deformation, respectively. In fact, unless an additional loading or boundary condition is specified, the cracked bodies cannot be in equilibrium. Other types of specimen are usually used. For instance, a long cylinder of a circular cross-section with a longitudinal slit under torsion (see Figure 3.2) can be used to produce a pure Mode III crack deformation.

3.2 METHOD OF COMPLEX POTENTIAL FOR PLANE ELASTICITY (THE KOLOSOV-MUSKHELISHVILI FORMULAS)

Among various mathematical methods in plane elasticity, the complex potential function method by Kolosov and Muskhelishvili [3-2] are one of the powerful and convenient methods to treat two-dimensional crack problems. In the complex potential method, stresses and displacements are expressed in terms of analytic functions of complex variables. The problem of obtaining stresses and displacements around a crack tip is converted to finding some analytic functions subjected to appropriate boundary conditions. A brief introduction of the general formulation of the Kolosov and Muskhelishvili complex potentials is given in this section.

3.2.1 Basic Equations of Plane Elasticity and Airy Stress Function

The basic equations of elasticity consist of equilibrium equations of stresses, strain-displacement relations, and Hooke's law that relates stresses and strains. In plane elasticity (plane strain and plane stress), the equilibrium equations are (body forces are absent)

$$\begin{aligned} \frac{\partial \sigma_{xx}}{\partial x} + \frac{\partial \sigma_{xy}}{\partial y} &= 0 \\ \frac{\partial \sigma_{xy}}{\partial x} + \frac{\partial \sigma_{yy}}{\partial y} &= 0 \end{aligned} \tag{3.2}$$

where σ_{xx}, σ_{yy}, and σ_{xy} are stresses, and (x,y) are Cartesian coordinates. The strains and the displacements are related by

$$e_{xx} = \frac{\partial u_x}{\partial x}, \quad e_{yy} = \frac{\partial u_y}{\partial y}, \quad e_{xy} = \frac{1}{2}\left(\frac{\partial u_x}{\partial y} + \frac{\partial u_y}{\partial x}\right) \tag{3.3}$$

where e_{xx}, e_{yy}, and e_{xy} are tensorial strain components, and u_x and u_y are displacements. The stress–strain relations are given by

$$\begin{aligned} \sigma_{xx} &= \lambda^* \left(e_{xx} + e_{yy}\right) + 2\mu e_{xx} \\ \sigma_{yy} &= \lambda^* \left(e_{xx} + e_{yy}\right) + 2\mu e_{yy} \\ \sigma_{xy} &= 2\mu e_{xy} \end{aligned} \tag{3.4}$$

or inversely

$$\begin{aligned} e_{xx} &= \frac{1}{2\mu}\left[\sigma_{xx} - \frac{\lambda^*}{2\left(\lambda^* + \mu\right)}\left(\sigma_{xx} + \sigma_{yy}\right)\right] \\ e_{yy} &= \frac{1}{2\mu}\left[\sigma_{yy} - \frac{\lambda^*}{2\left(\lambda^* + \mu\right)}\left(\sigma_{xx} + \sigma_{yy}\right)\right] \\ e_{xy} &= \frac{1}{2\mu}\sigma_{xy} \end{aligned} \tag{3.5}$$

where μ is the shear modulus and

$$\lambda^* = \frac{3-\kappa}{\kappa - 1}\mu$$

in which

$$\kappa = \begin{cases} 3 - 4\nu & \text{for plane strain} \\ \dfrac{3-\nu}{1+\nu} & \text{for plane stress} \end{cases} \tag{3.6}$$

In the previous relation, ν is Poisson's ratio. The compatibility equation of strains can be obtained from Eq. (3.3) by eliminating the displacements as follows:

$$\frac{\partial^2 e_{xx}}{\partial y^2} + \frac{\partial^2 e_{yy}}{\partial x^2} = 2\frac{\partial^2 e_{xy}}{\partial x \partial y} \tag{3.7}$$

By using the stress–strain relations Eq. (3.5) together with the equations of equilibrium Eq. (3.2), the compatibility condition Eq. (3.7) can be expressed in terms of stresses as

$$\nabla^2(\sigma_{xx} + \sigma_{yy}) = 0 \tag{3.8}$$

where

$$\nabla^2 = \frac{\partial^2}{\partial x^2} + \frac{\partial^2}{\partial y^2}$$

is the Laplace operator.

The Airy stress function ϕ is defined through

$$\sigma_{xx} = \frac{\partial^2 \phi}{\partial y^2}, \quad \sigma_{xy} = -\frac{\partial^2 \phi}{\partial x \partial y}, \quad \sigma_{yy} = \frac{\partial^2 \phi}{\partial x^2} \tag{3.9}$$

Using these relations, the equilibrium equations in Eq. (3.2) are automatically satisfied, and the compatibility Eq. (3.8) becomes

$$\nabla^4 \phi = \nabla^2 \nabla^2 \phi = 0 \tag{3.10}$$

where

$$\nabla^4 = \nabla^2 \nabla^2 = \frac{\partial^4}{\partial x^4} + 2\frac{\partial^4}{\partial x^2 \partial y^2} + \frac{\partial^4}{\partial y^4}$$

is the biharmonic operator. Any function ϕ satisfying Eq. (3.10) is called a biharmonic function. A harmonic function f satisfies $\nabla^2 f = 0$. Thus, if f is harmonic, it is also biharmonic. However, the converse is not true. Once the Airy stress function is known, the stresses can be obtained by Eq. (3.9) and strains and displacements obtained through Eqs. (3.5) and (3.3), respectively.

3.2.2 Analytic Functions and Cauchy-Riemann Equations

In a Cartesian coordinate system (x, y), the complex variable z and its conjugate $\bar{z}$ are defined as

$$z = x + iy$$

and

$$\bar{z} = x - iy$$

respectively, where $i = \sqrt{-1}$. They can also be expressed in polar coordinates (r, θ) as

$$z = r(\cos\theta + i\sin\theta) = re^{i\theta}$$

and

$$\bar{z} = r(\cos\theta - i\sin\theta) = re^{-i\theta}$$

respectively.

Consider a function of the complex variable z, $f(z)$. The derivative of $f(z)$ with respect to z is by definition

$$\frac{df(z)}{dz} = \lim_{\Delta z \to 0} \frac{f(z+\Delta z) - f(z)}{\Delta z}$$

If $f(z)$ has a derivative at point z_0 and also at each point in some neighborhood of z_0, then $f(z)$ is said to be analytic at z_0. The complex function $f(z)$ can be expressed in the form

$$f(z) = u(x,y) + iv(x,y)$$

where u and v are real functions. If $f(z)$ is analytic, we have

$$\frac{\partial}{\partial x} f(z) = f'(z)\frac{\partial z}{\partial x} = f'(z)$$

and

$$\frac{\partial}{\partial y} f(z) = f'(z)\frac{\partial z}{\partial y} = if'(z)$$

where a prime stands for differentiation with respect to z. Thus,

$$\frac{\partial}{\partial x} f(z) = -i\frac{\partial}{\partial y} f(z)$$

or

$$\frac{\partial u}{\partial x} + i\frac{\partial v}{\partial x} = \frac{\partial v}{\partial y} - i\frac{\partial u}{\partial y}$$

From this equation, we obtain the Cauchy-Riemann equations:

$$\frac{\partial u}{\partial x} = \frac{\partial v}{\partial y}, \quad \frac{\partial u}{\partial y} = -\frac{\partial v}{\partial x} \tag{3.11}$$

These equations can also be shown to be sufficient for $f(z)$ to be analytic.

From the Cauchy-Riemann equations it is easy to derive the following:

$$\nabla^2 u = \nabla^2 v = 0$$

that is, the real and imaginary parts of an analytic function are harmonic.

3.2.3 Complex Potential Representation of the Airy Stress Function

The Airy stress function ϕ is biharmonic according to Eq. (3.10). Introduce a function P by

$$\nabla^2 \phi = P \tag{3.12}$$

then

$$\nabla^2 P = \nabla^2 \nabla^2 \phi = 0$$

This simply says that P is a harmonic function. Hence,

$$P = \text{Real part of } f(z) \equiv \text{Re}\{f(z)\}$$

where $f(z)$ is an analytic function and can be expressed as

$$f(z) = P + iQ$$

Let

$$\psi(z) = \frac{1}{4}\int f(z)dz = p + iq$$

then ψ is also analytic and its derivative is given by

$$\psi'(z) = \frac{1}{4}f(z)$$

According to the Cauchy-Riemann equations, we have

$$\psi'(z) = \frac{\partial p}{\partial x} + i\frac{\partial q}{\partial x} = \frac{\partial q}{\partial y} - i\frac{\partial p}{\partial y}$$

A relation between P and p (or q) can then be obtained:

$$P = 4\frac{\partial p}{\partial x} = 4\frac{\partial q}{\partial y} \tag{3.13}$$

Consider the function $\phi - (xp + yq)$. It can be shown that

$$\nabla^2[\phi - (xp + yq)] = 0$$

Thus, $\phi - (xp + yq)$ is harmonic and is a real (or imaginary) part of an analytic function, say $\chi(z)$, that is,

$$\phi - (xp + yq) = \text{Re}\{\chi(z)\}$$

Using the relation

$$xp + yq = \text{Re}\{\bar{z}\psi(z)\}$$

we obtain the complex potential representation of the Airy stress function

$$\begin{aligned} \phi &= \text{Re}\{\bar{z}\psi(z) + \chi(z)\} \\ 2\phi(x,y) &= \bar{z}\psi(z) + z\overline{\psi(z)} + \chi(z) + \overline{\chi(z)} \end{aligned} \tag{3.14}$$

3.2.4 Stress and Displacement

From the definition of the Airy stress function we obtain

$$\begin{aligned}\sigma_{xx}+i\sigma_{xy}&=\frac{\partial^2\phi}{\partial y^2}-i\frac{\partial^2\phi}{\partial x\partial y}=-i\frac{\partial}{\partial y}\left(\frac{\partial\phi}{\partial x}+i\frac{\partial\phi}{\partial y}\right)\\ \sigma_{yy}-i\sigma_{xy}&=\frac{\partial^2\phi}{\partial x^2}+i\frac{\partial^2\phi}{\partial x\partial y}=\frac{\partial}{\partial x}\left(\frac{\partial\phi}{\partial x}+i\frac{\partial\phi}{\partial y}\right)\end{aligned} \tag{3.15}$$

Note that for an analytic function $f(z)$ we have

$$\begin{aligned}\frac{\partial f(z)}{\partial x}&=f'(z)\frac{\partial z}{\partial x}=f'(z)\\ \frac{\partial\overline{f(z)}}{\partial x}&=\overline{\left(\frac{\partial f(z)}{\partial x}\right)}=\overline{f'(z)}\\ \frac{\partial f(z)}{\partial y}&=f'(z)\frac{\partial z}{\partial y}=if'(z)\\ \frac{\partial\overline{f(z)}}{\partial y}&=\overline{\left(\frac{\partial f(z)}{\partial y}\right)}=-i\overline{f'(z)}\end{aligned}$$

Using the preceding relations together with Eq. (3.14), we obtain

$$\frac{\partial\phi}{\partial x}+i\frac{\partial\phi}{\partial y}=\psi(z)+z\overline{\psi'(z)}+\overline{\chi'(z)} \tag{3.16}$$

Substitution of the relation in (3.16) in Eq. (3.15) leads to

$$\begin{aligned}\sigma_{xx}+i\sigma_{xy}&=\psi'(z)+\overline{\psi'(z)}-z\overline{\psi''(z)}-\overline{\chi''(z)}\\ \sigma_{yy}-i\sigma_{xy}&=\psi'(z)+\overline{\psi'(z)}+z\overline{\psi''(z)}+\overline{\chi''(z)}\end{aligned} \tag{3.17}$$

Summing the two equations in Eq. (3.17), we have

$$\sigma_{xx}+\sigma_{yy}=2[\psi'(z)+\overline{\psi'(z)}]=4\,\mathrm{Re}[\psi'(z)] \tag{3.18}$$

Subtracting the first equation from the second one in Eq. (3.17), we obtain

$$\sigma_{yy}-\sigma_{xx}-2i\sigma_{xy}=2z\overline{\psi''(z)}+2\overline{\chi''(z)}$$

The equation above can be rewritten in the following form by taking the conjugate of the quantities on both sides:

$$\sigma_{yy}-\sigma_{xx}+2i\sigma_{xy}=2[\bar{z}\psi''(z)+\chi''(z)] \tag{3.19}$$

Equations (3.18) and (3.19) are the convenient analytic function representations of stresses.

We now turn to the complex potential representation of displacements. Substituting the strain-displacement relations Eq. (3.3) and the stresses in Eq. (3.9) into the

stress–strain relations Eq. (3.5) yields

$$\begin{aligned} 2\mu\frac{\partial u_x}{\partial x} &= \frac{\partial^2\phi}{\partial y^2} - \frac{\lambda^*}{2(\lambda^*+\mu)}\nabla^2\phi \\ 2\mu\frac{\partial u_y}{\partial y} &= \frac{\partial^2\phi}{\partial x^2} - \frac{\lambda^*}{2(\lambda^*+\mu)}\nabla^2\phi \\ \mu\left(\frac{\partial u_x}{\partial y} + \frac{\partial u_y}{\partial x}\right) &= -\frac{\partial^2\phi}{\partial x\partial y} \end{aligned} \tag{3.20}$$

From Eqs. (3.12) and (3.13) we have

$$\nabla^2\phi = P = 4\frac{\partial p}{\partial x} = 4\frac{\partial q}{\partial y}$$

Substitution of this equation into the first two equations in Eq. (3.20) yields

$$\begin{aligned} 2\mu\frac{\partial u_x}{\partial x} &= -\frac{\partial^2\phi}{\partial x^2} + \frac{2(\lambda^*+2\mu)}{\lambda^*+\mu}\frac{\partial p}{\partial x} \\ 2\mu\frac{\partial u_y}{\partial y} &= -\frac{\partial^2\phi}{\partial y^2} + \frac{2(\lambda^*+2\mu)}{\lambda^*+\mu}\frac{\partial q}{\partial y} \end{aligned}$$

Integrating the preceding equations, we obtain

$$\begin{aligned} 2\mu u_x &= -\frac{\partial\phi}{\partial x} + \frac{2(\lambda^*+2\mu)}{\lambda^*+\mu}p + f_1(y) \\ 2\mu u_y &= -\frac{\partial\phi}{\partial y} + \frac{2(\lambda^*+2\mu)}{\lambda^*+\mu}q + f_2(x) \end{aligned} \tag{3.21}$$

Substituting these expressions in the third equation in Eq. (3.20), we can conclude that $f_1(y)$ and $f_2(x)$ represent rigid body displacements and thus can be neglected. Rewrite Eq. (3.21) in complex form:

$$2\mu(u_x + iu_y) = -\left(\frac{\partial\phi}{\partial x} + i\frac{\partial\phi}{\partial y}\right) + \frac{2(\lambda^*+2\mu)}{\lambda^*+\mu}\psi(z)$$

Using Eq. (3.16) in the previous expression, we arrive at the complex potential representation of displacements:

$$2\mu(u_x + iu_y) = \kappa\psi(z) - z\overline{\psi'(z)} - \overline{\chi'(z)} \tag{3.22}$$

In deriving Eq. (3.22), the relation

$$\kappa = \frac{\lambda^*+3\mu}{\lambda^*+\mu}$$

is used. Equations (3.18), (3.19), and (3.22) are the Kolosov-Muskhelishvili formulas.

3.3 WESTERGAARD FUNCTION METHOD

The Kolosov-Muskhelishvili formulas hold for general plane elasticity problems. In applications to crack problems, however, the three basic fracture modes discussed in Section 3.1 possess symmetry or antisymmetry properties. The Westergaard function method [3-3, 3-4] is more convenient for discussing these basic crack problems. We will introduce the Westergaard functions using the general Kolosov-Muskhelishvili formulas, which are rewritten here for convenience:

$$\sigma_{xx} + \sigma_{yy} = 4\,\mathrm{Re}\{\psi'(z)\} \tag{3.23}$$

$$\sigma_{yy} - \sigma_{xx} + 2i\sigma_{xy} = 2\{\bar{z}\psi''(z) + \chi''(z)\} \tag{3.24}$$

$$2\mu(u_x + iu_y) = \kappa\psi(z) - z\overline{\psi'(z)} - \overline{\chi'(z)} \tag{3.25}$$

3.3.1 Symmetric Problems (Mode I)

Consider an infinite plane with cracks along the x-axis. If the external loads are symmetric with respect to the x-axis, then $\sigma_{xy} = 0$ along $y = 0$. From Eq. (3.24), we have

$$\mathrm{Im}\{\bar{z}\psi''(z) + \chi''(z)\} = 0 \quad \text{at } y = 0 \tag{3.26}$$

The preceding equation can be satisfied if and only if

$$\chi''(z) + z\psi''(z) + A = 0 \tag{3.27}$$

in which A is a real constant.

Proof

It is clear that Eq. (3.27) leads to Eq. (3.26) because $z = \bar{z}$ at $y = 0$. For the converse case, consider

$$\chi''(z) + z\psi''(z) = -A(z) \tag{3.28}$$

We now prove from Eq. (3.26) that $A(z)$ is a real constant. First, $A(z)$ is analytic since χ'' and $z\psi''$ are analytic. Second, $A(z)$ is bounded in the entire plane according to Eq. (3.24) (stresses are finite everywhere except at crack tips) and the general asymptoptic solutions of $\psi(z)$ and $\chi(z)$ at crack tips (see Section 3.6). $A(z)$ is thus a constant ($= A$) by Liouville's theorem. Substituting Eq. (3.28) into the left side of Eq. (3.26), we have

$$\mathrm{Im}\{(\bar{z} - z)\psi''(z) - A\} = \mathrm{Im}\{-2iy\psi''(z) - A\} = 0 \quad \text{at } y = 0$$

or

$$\mathrm{Im}\{-A\} = 0$$

Hence, we can conclude that

$$A = \text{real constant}$$

Because $\psi(z)$ and $\chi(z)$ are related according to Eq. (3.27), stresses and displacements may be expressed by only one of the two analytic functions. From Eq. (3.27), we obtain

$$\chi''(z) = -z\psi'' - A$$

Substituting this equation into Eqs. (3.23) through (3.25) and solving the resulting equations, we have

$$\begin{aligned}
\sigma_{xx} &= 2\,\mathrm{Re}\{\psi'\} - 2y\,\mathrm{Im}\{\psi''\} + A \\
\sigma_{yy} &= 2\,\mathrm{Re}\{\psi'\} + 2y\,\mathrm{Im}\{\psi''\} - A \\
\sigma_{xy} &= -2y\,\mathrm{Re}\{\psi''\} \\
2\mu u_x &= (\kappa - 1)\,\mathrm{Re}\{\psi\} - 2y\,\mathrm{Im}\{\psi'\} + Ax \\
2\mu u_y &= (\kappa + 1)\,\mathrm{Im}\{\psi\} - 2y\,\mathrm{Re}\{\psi'\} - Ay
\end{aligned} \tag{3.29}$$

Define

$$\psi' = \frac{1}{2}(Z_I + A)$$

Thus,

$$\begin{aligned}
\psi &= \frac{1}{2}(\hat{Z}_I + Az) \\
\psi'' &= \frac{1}{2}Z_I'
\end{aligned}$$

where $\hat{Z}_I' \equiv Z_I$. The use of these two equations in Eq. (3.29) results in

$$\begin{aligned}
\sigma_{xx} &= \mathrm{Re}\{Z_I\} - y\,\mathrm{Im}\{Z_I'\} + 2A \\
\sigma_{yy} &= \mathrm{Re}\{Z_I\} + y\,\mathrm{Im}\{Z_I'\} \\
\sigma_{xy} &= -y\,\mathrm{Re}\{Z_I'\} \\
2\mu u_x &= \frac{(\kappa - 1)}{2}\,\mathrm{Re}\{\hat{Z}_I\} - y\,\mathrm{Im}\{Z_I\} + \frac{1}{2}(\kappa + 1)Ax \\
2\mu u_y &= \frac{(\kappa + 1)}{2}\,\mathrm{Im}\{\hat{Z}_I\} - y\,\mathrm{Re}\{Z_I\} + \frac{1}{2}(\kappa - 3)Ay
\end{aligned} \tag{3.30}$$

Z_I is the so-called Westergaard function for Mode I problems. It is obvious that the stress field associated with A is a uniform uniaxial stress $\sigma_{xx} = 2A$. This stress field does not add to the stress singularity at the crack tip.

From Eq. (3.30), we note that

$$\sigma_{xx} - \sigma_{yy} = 2A = \text{constant} \quad \text{at } y = 0$$

For the case where uniform tension is applied in the y-direction; that is, $\sigma_{xx} = 0$ and $\sigma_{yy} = \sigma_0$, $A = -\sigma_0/2$. If the panel is subjected to biaxial tensions of equal magnitude, then $A = 0$.

The Airy stress function corresponding to the constant stress field $\sigma_{xx} = 2A = \partial^2\phi/\partial y^2$ is given by

$$\phi = Ay^2$$

It can be easily verified that the stresses and displacements of Eq. (3.30) are derived from the stress function (see Problem 3.3)

$$\phi = \text{Re}\{\widehat{\widehat{Z}}_I\} + y\,\text{Im}\{\widehat{Z}_I\} + Ay^2$$

The function Z_I is usually associated with Westergaard [3-3], who used it to solve the contact pressure distribution resulting from the contact of many surfaces and some crack problems. In its original form used by Westergaard, $A = 0$. In 1957, Irwin [3-1] used Westergaard's solutions to obtain the stress field at the crack tip and related that to the strain energy release rate.

3.3.2 Skew-Symmetric Problems (Mode II)

For loads that are skew-symmetric with respect to the crack line (x-axis), the normal stress σ_{yy} is zero along $y = 0$. From Eqs. (3.23) and (3.24), this condition gives rise to

$$\text{Re}\{2\psi'(z) + \bar{z}\psi''(z) + \chi''\} = 0 \quad \text{at } y = 0 \tag{3.31}$$

Following the same procedure described for the symmetric problem, we obtain

$$\chi''(z) + 2\psi'(z) + z\psi''(z) + iB = 0$$

in which B is a real constant. Using this equation, $\chi(z)$ can be eliminated in Eqs. (3.23) through (3.25) and we have

$$\begin{aligned}
\sigma_{xx} &= 4\,\text{Re}\{\psi'(z)\} - 2y\,\text{Im}\{\psi''(z)\} \\
\sigma_{yy} &= 2y\,\text{Im}\{\psi''(z)\} \\
\sigma_{xy} &= -2\,\text{Im}\{\psi'(z)\} - 2y\,\text{Re}\{\psi''(z)\} - B \\
2\mu u_x &= (\kappa + 1)\,\text{Re}\{\psi(z)\} - 2y\,\text{Im}\{\psi'(z)\} - By \\
2\mu u_y &= (\kappa - 1)\text{Im}\{\psi(z)\} - 2y\,\text{Re}\{\psi'(z)\} - Bx
\end{aligned} \tag{3.32}$$

Define an analytic function $\Psi(z)$ by

$$\Psi'(z) = \psi'(z) + \frac{i}{2}B$$

Then

$$\Psi(z) = \psi(z) + \frac{i}{2}Bz$$
$$\Psi''(z) = \psi''(z)$$

Substituting these definitions into Eq. (3.32), we obtain

$$\begin{aligned}
\sigma_{xx} &= 4\,\mathrm{Re}\{\Psi'(z)\} - 2y\,\mathrm{Im}\{\Psi''(z)\} \\
\sigma_{yy} &= 2y\,\mathrm{Im}\{\Psi''\} \\
\sigma_{xy} &= -2\,\mathrm{Im}\{\Psi'(z)\} - 2y\,\mathrm{Re}\{\Psi''(z)\} \qquad (3.33)\\
2\mu u_x &= (\kappa+1)\mathrm{Re}\{\Psi(z)\} - 2y\,\mathrm{Im}\{\Psi'(z)\} + \frac{\kappa+1}{2}By \\
2\mu u_x &= (\kappa-1)\mathrm{Im}\{\Psi(z)\} - 2y\,\mathrm{Re}\{\Psi'(z)\} - \frac{\kappa+1}{2}Bx
\end{aligned}$$

The last term in the displacement components u_x and u_y represents a rigid body rotation. Define Westergaard function Z_{II} as

$$Z_{II} = 2i\Psi'(z)$$

Then Eq. (3.33) becomes

$$\begin{aligned}
\sigma_{xx} &= 2\mathrm{Im}\{Z_{II}\} + y\,\mathrm{Re}\{Z'_{II}\} \\
\sigma_{yy} &= -y\,\mathrm{Re}\{Z'_{II}\} \\
\sigma_{xy} &= \mathrm{Re}\{Z_{II}\} - y\,\mathrm{Im}\{Z'_{II}\} \qquad (3.34)\\
2\mu u_x &= \frac{1}{2}(\kappa+1)\mathrm{Im}\{\widehat{Z}_{II}\} + y\,\mathrm{Re}\{Z_{II}\} + \frac{\kappa+1}{2}By \\
2\mu u_y &= -\frac{1}{2}(\kappa-1)\mathrm{Re}\{\widehat{Z}_{II}\} - y\,\mathrm{Im}\{Z_{II}\} - \frac{\kappa+1}{2}Bx
\end{aligned}$$

Thus, the Westergaard function $Z_{II}(z)$ provides the general solution for the skew-symmetric problems.

We conclude that any plane elasticity problem involving collinear straight cracks in an infinite plane can be completely solved by the stress function

$$\phi = \mathrm{Re}\{\widehat{\widehat{Z}}_I\} + y\mathrm{Im}\{\widehat{Z}_I\} - y\,\mathrm{Re}\{\widehat{Z}_{II}\} + Ay^2$$

This is an alternative form to Eq. (3.14). The advantage of using the Westergaard functions is that the two modes of fracture are represented separately by two analytic functions.

3.4 SOLUTIONS BY THE WESTERGAARD FUNCTION METHOD

A center crack in an infinite plate under uniform remote loading is perhaps the best example to introduce the basic concepts of stress intensity factor and near-tip stress and deformation fields. In this section, the Westergaard function method is used to find the elasticity solutions for an infinite plane with a center crack under uniform biaxial tension, in-plane shear, and antiplane shear loading, respectively. We will see that the near-tip singular stress fields can be easily extracted from the complete solutions and the stress intensity factors can be obtained from the solutions using the definition in Eq. (3.1). Furthermore, stress intensity factors may also be conveniently determined directly from the general Kolosov-Muskhelishvili potentials or Westergaard functions.

3.4.1 Mode I Crack

One of the most typical crack problems in fracture mechanics is an infinite plane with a line crack of length $2a$ subjected to biaxial stress σ_0 at infinity, as shown in Figure 3.3. In practice, if the crack length is much smaller than any in-plane size of the concerned elastic body, the region may be mathematically treated as an infinite plane with a finite crack. The problem is Mode I since the loads are symmetric with respect to the crack line.

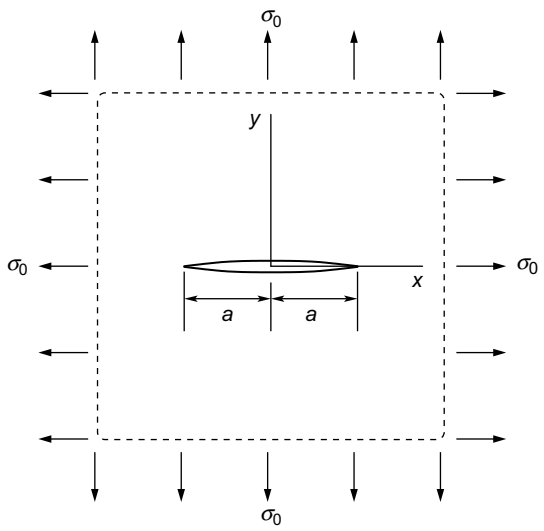

FIGURE 3.3

A crack in an infinite elastic plane subjected to biaxial tension.

Solution of Stresses

The boundary conditions of the crack problem are

$$\begin{aligned} &\sigma_{xy} = \sigma_{yy} = 0 \quad \text{at } |x| \le a \text{ and } y = 0 \quad \text{(crack surfaces)} \\ &\sigma_{xx} = \sigma_{yy} = \sigma_0,\ \sigma_{xy} = 0 \quad \text{at } x^2 + y^2 \to \infty \end{aligned} \tag{3.35}$$

The solution to the preceding boundary value problem was given by Westergaard [3-3] with

$$Z_I(z) = \frac{\sigma_0 z}{\sqrt{z^2 - a^2}}, \quad A = 0 \tag{3.36}$$

Since all the equations of plane elasticity are automatically satisfied, we only need to verify that the stresses obtained by Eq. (3.30) with Z_I given in Eq. (3.36) satisfy the boundary conditions Eq. (3.35).

To find the explicit expressions of the stress field, it is more convenient to use the polar coordinates shown in Figure 3.4. The following relations are obvious:

$$\begin{aligned} z &= re^{i\theta} \\ z - a &= r_1 e^{i\theta_1} \\ z + a &= r_2 e^{i\theta_2} \end{aligned} \tag{3.37}$$

In terms of these polar coordinates, the function Z_I becomes

$$\begin{aligned} Z_I &= \frac{\sigma_0 z}{\sqrt{z+a}\sqrt{z-a}} \\ &= \frac{\sigma_0 r}{\sqrt{r_1 r_2}} \exp i\left(\theta - \frac{1}{2}\theta_1 - \frac{1}{2}\theta_2\right) \end{aligned} \tag{3.38}$$

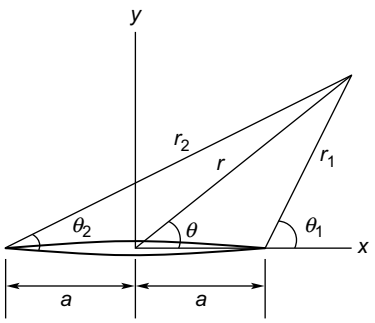

FIGURE 3.4

Polar coordinate systems.

The derivative of Z_I is obtained as

$$Z_I' = \frac{\sigma_0}{\sqrt{z^2-a^2}} - \frac{\sigma_0 z^2}{(z^2-a^2)^{3/2}} = -\frac{\sigma_0 a^2}{(z^2-a^2)^{3/2}}$$
$$= -\frac{\sigma_0 a^2}{(r_1 r_2)^{3/2}} \exp\left(-i\frac{3}{2}(\theta_1+\theta_2)\right) \tag{3.39}$$

It follows from Eqs. (3.38) and (3.39) that

$$\mathrm{Re}\{Z_I\} = \frac{\sigma_0 r}{\sqrt{r_1 r_2}} \cos\left(\theta - \frac{1}{2}\theta_1 - \frac{1}{2}\theta_2\right)$$
$$\mathrm{Re}\{Z_I'\} = \frac{-\sigma_0 a^2}{(r_1 r_2)^{3/2}} \cos\frac{3}{2}(\theta_1+\theta_2)$$
$$\mathrm{Im}\{Z_I'\} = \frac{\sigma_0 a^2}{(r_1 r_2)^{3/2}} \sin\frac{3}{2}(\theta_1+\theta_2)$$

Using these expressions, the normal stress σ_{xx} is obtained as

$$\sigma_{xx} = \mathrm{Re}\{Z_I\} - y\,\mathrm{Im}\{Z_I'\}$$
$$= \frac{\sigma_0 r}{\sqrt{r_1 r_2}} \cos\left(\theta - \frac{1}{2}\theta_1 - \frac{1}{2}\theta_2\right) - \frac{\sigma_0 a^2}{(r_1 r_2)^{3/2}} r\sin\theta \sin\frac{3}{2}(\theta_1+\theta_2)$$
$$= \frac{\sigma_0 r}{\sqrt{r_1 r_2}} \left[\cos\left(\theta - \frac{1}{2}\theta_1 - \frac{1}{2}\theta_2\right) - \frac{a^2}{r_1 r_2}\sin\theta\sin\frac{3}{2}(\theta_1+\theta_2)\right] \tag{3.40}$$

Similarly, the other two stress components can be obtained:

$$\sigma_{yy} = \frac{\sigma_0 r}{\sqrt{r_1 r_2}} \left[\cos\left(\theta - \frac{1}{2}\theta_1 - \frac{1}{2}\theta_2\right) + \frac{a^2}{r_1 r_2}\sin\theta\sin\frac{3}{2}(\theta_1+\theta_2)\right] \tag{3.41}$$

$$\sigma_{xy} = \frac{\sigma_0 r}{\sqrt{r_1 r_2}} \left[\frac{a^2}{r_1 r_2}\sin\theta\cos\frac{3}{2}(\theta_1+\theta_2)\right] \tag{3.42}$$

Using these stress expressions, it is easy to show that the tractions (σ_{yy} and σ_{xy}) on the crack surface ($\theta_1 = \pi, \theta_2 = 0, \theta = 0, \pi$) vanish completely.

At large distances ($r \to \infty$) from the crack it is easily seen that

$$r_1 \approx r_2 \approx r \to \infty$$
$$\theta_1 \approx \theta_2 \approx \theta$$

and consequently that

$$\sigma_{xx} = \sigma_0, \quad \sigma_{yy} = \sigma_0, \quad \sigma_{xy} = 0$$

Thus, the boundary conditions are satisfied everywhere. Equations (3.40) through (3.42) are the complete solution of the stress field in the entire cracked plane.

The Near-Tip Solution

In fracture mechanics, crack growth is controlled by the stresses and deformations around the crack tip. We thus study the near-tip asymptotic stress field. In the vicinity of the crack tip (say the right tip), we have

$$\frac{r_1}{a} \ll 1, \quad \theta \approx 0, \quad \theta_2 \approx 0$$

$$r \approx a, \quad r_2 \approx 2a$$

$$\sin\theta \approx \frac{r_1}{a}\sin\theta_1$$

$$\sin\frac{3}{2}(\theta_1+\theta_2) \approx \sin\frac{3}{2}\theta_1$$

$$\cos\left(\theta - \frac{1}{2}\theta_1 - \frac{1}{2}\theta_2\right) \approx \cos\frac{1}{2}\theta_1$$

$$\cos\frac{3}{2}(\theta_1+\theta_2) \approx \cos\frac{3}{2}\theta_1$$

By using the preceding asymptotic expressions, Eq. (3.40) reduces to

$$\begin{aligned}\sigma_{xx} &= \frac{\sigma_0 a}{\sqrt{2ar_1}}\left(\cos\frac{1}{2}\theta_1 - \frac{a^2}{2ar_1}\frac{r_1}{a}\sin\theta_1\sin\frac{3}{2}\theta_1\right)\\ &= \frac{\sigma_0\sqrt{a}}{\sqrt{2r_1}}\left(\cos\frac{1}{2}\theta_1 - \frac{1}{2}\sin\theta_1\sin\frac{3}{2}\theta_1\right)\\ &= \frac{\sigma_0\sqrt{a}}{\sqrt{2r_1}}\cos\frac{1}{2}\theta_1\left(1 - \sin\frac{1}{2}\theta_1\sin\frac{3}{2}\theta_1\right)\end{aligned}$$

Similarly,

$$\sigma_{yy} = \frac{\sigma_0\sqrt{a}}{\sqrt{2r_1}}\cos\frac{1}{2}\theta_1\left(1 + \sin\frac{1}{2}\theta_1\sin\frac{3}{2}\theta_1\right)$$

$$\sigma_{xy} = \frac{\sigma_0\sqrt{a}}{\sqrt{2r_1}}\sin\frac{1}{2}\theta_1\cos\frac{1}{2}\theta_1\cos\frac{3}{2}\theta_1$$

Along the crack extended line ($\theta = \theta_1 = \theta_2 = 0$), these near-tip stresses are

$$\sigma_{yy} = \frac{\sigma_0\sqrt{\pi a}}{\sqrt{2\pi r_1}}$$

$$\sigma_{xy} = 0$$

Comparing the previous stresses with Eq. (3.1) in Section 3.1, we have the Mode I stress intensity factor K_I for the crack problem as

$$K_I = \sigma_0 \sqrt{\pi a} \tag{3.43}$$

and the Mode II stress intensity factor $K_{II} = 0$.

If the origin of the coordinate system (r,θ) is located at the crack tip, then the stress field near the crack tip can be written in terms of the stress intensity factor K_I as

$$\begin{aligned}
\sigma_{xx} &= \frac{K_I}{\sqrt{2\pi r}} \cos\frac{1}{2}\theta \left(1 - \sin\frac{1}{2}\theta \sin\frac{3}{2}\theta\right) \\
\sigma_{yy} &= \frac{K_I}{\sqrt{2\pi r}} \cos\frac{1}{2}\theta \left(1 + \sin\frac{1}{2}\theta \sin\frac{3}{2}\theta\right) \\
\sigma_{xy} &= \frac{K_I}{\sqrt{2\pi r}} \sin\frac{1}{2}\theta \cos\frac{1}{2}\theta \cos\frac{3}{2}\theta
\end{aligned} \tag{3.44}$$

Following the same procedures, the near-tip displacements are obtained as

$$\begin{aligned}
u_x &= \frac{K_I}{8\mu\pi} \sqrt{2\pi r} \left[(2\kappa - 1)\cos\frac{\theta}{2} - \cos\frac{3\theta}{2}\right] \\
u_y &= \frac{K_I}{8\mu\pi} \sqrt{2\pi r} \left[(2\kappa + 1)\sin\frac{\theta}{2} - \sin\frac{3\theta}{2}\right]
\end{aligned} \tag{3.45}$$

Equation (3.44) shows that stresses have an inverse square root singularity at the crack tip and the intensity of the singular stress field is described by the stress intensity factor.

Equations (3.44) and (3.45) are derived for a crack in an infinite plane subjected to remote biaxial tension. It will be seen in Section 3.7 that these expressions for the near-tip stresses and displacements hold for any cracked body undergoing Mode I deformations. The difference is only the value of the stress intensity factor. Hence, once the stress σ_{yy} along the crack extended line is known, the Mode I stress intensity factor can be obtained from

$$K_I = \lim_{r \to 0} \sqrt{2\pi r}\, \sigma_{yy}(\theta = 0) \tag{3.46}$$

Crack Surface Displacement

Besides the near-tip stress field, the displacements of crack faces are also relavent to crack growth. Under Mode I deformation conditions, the crack surfaces open up, which is quantified by the vertical displacement component u_y. For the problem shown in Figure 3.3, we already have

$$Z_I = \frac{\sigma_0 z}{\sqrt{z^2 - a^2}}$$

and

$$\hat{Z}_I = \sigma_0 \sqrt{z^2 - a^2}$$

In terms of the polar coordinates defined in Eq. (3.37) and Figure 3.4, the function $\hat{Z}_I$ can be expressed as

$$\hat{Z}_I = \sigma_0 \sqrt{r_1 r_2} e^{\frac{1}{2} i(\theta_1 + \theta_2)}$$

The corresponding vertical displacement is obtained from the last equation of Eq. (3.30):

$$\begin{aligned} 4\mu u_y &= (\kappa + 1)\mathrm{Im}\hat{Z}_I \\ &= (\kappa + 1)\sigma_0 \sqrt{r_1 r_2} \sin \frac{1}{2}(\theta_1 + \theta_2) \end{aligned}$$

The upper crack surface corresponds to $\theta_1 = \pi$, $\theta_2 = 0$ and the lower surface is $\theta_1 = -\pi$, $\theta_2 = 0$. The displacement of the upper crack surface is thus given by

$$u_y = \frac{\kappa + 1}{4\mu} \sigma_0 \sqrt{r_1 r_2} = \frac{\kappa + 1}{4\mu} \sigma_0 \sqrt{a^2 - x^2} \tag{3.47}$$

Near the crack tip, $r_1 \ll a$, $r_2 \approx 2a$, and Eq. (3.47) reduces to

$$\begin{aligned} u_y &= \frac{\kappa + 1}{4\mu} \sigma_0 \sqrt{2a r_1} \\ &= \frac{\kappa + 1}{4\pi\mu} K_I \sqrt{2\pi r_1} \end{aligned}$$

which is consistent with Eq. (3.45).

3.4.2 Mode II Crack

Consider a cracked plate of infinite extent that is subjected to uniform shear stress τ_0 at infinity as shown in Figure 3.5. This is a basic Mode II problem with the following skew-symetric boundary conditions:

$$\begin{aligned} &\sigma_{xy} = 0,\ \sigma_{yy} = 0 \quad \text{at } |x| \le a \text{ and } y = 0 \quad \text{(crack surfaces)} \\ &\sigma_{xx} = \sigma_{yy} = 0, \sigma_{xy} = \tau_0 \quad \text{at } x^2 + y^2 \to \infty \end{aligned} \tag{3.48}$$

It can be shown that the following Westergaard function,

$$Z_{II}(z) = \frac{\tau_0 z}{\sqrt{z^2 - a^2}} \tag{3.49}$$

yields stresses that satisfy the boundary conditions Eq. (3.48) and, hence, yields the solution for the problem. The stress field can be computed according to Eqs. (3.34)

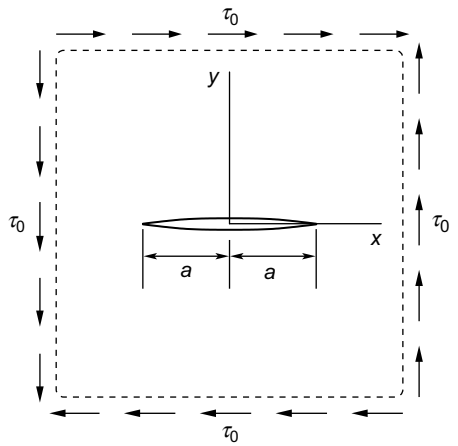

FIGURE 3.5

A crack in an infinite elastic plane subjected to pure in-plane shear.

and (3.49). Following the same procedure described for the Mode I crack and using the polar coordinates defined in Eq. (3.37) and Figure 3.4, we have the complete stress field,

$$\begin{aligned}
\sigma_{xx} &= \frac{\tau_0 r}{\sqrt{r_1 r_2}}\left[2\sin\left(\theta - \frac{1}{2}\theta_1 - \frac{1}{2}\theta_2\right) - \frac{a^2}{r_1 r_2}\sin\theta\cos\frac{3}{2}(\theta_1+\theta_2)\right] \\
\sigma_{yy} &= \frac{\tau_0 a^2 r}{(r_1 r_2)^{3/2}}\sin\theta\cos\frac{3}{2}(\theta_1+\theta_2) \\
\sigma_{xy} &= \frac{\tau_0 r}{\sqrt{r_1 r_2}}\left[\cos\left(\theta - \frac{1}{2}\theta_1 - \frac{1}{2}\theta_2\right) - \frac{a^2}{r_1 r_2}\sin\theta\sin\frac{3}{2}(\theta_1+\theta_2)\right]
\end{aligned} \tag{3.50}$$

Along the crack extended line ($\theta_1 = \theta_2 = \theta = 0$) and near the crack tip ($r_1/a \ll 1$), the stresses are

$$\begin{aligned}
\sigma_{yy} &= 0 \\
\sigma_{xy} &= \frac{\tau_0\sqrt{\pi a}}{\sqrt{2\pi r_1}}
\end{aligned}$$

Comparing these stresses with Eq. (3.1) in Section 3.1, we have the Mode II stress intensity factor K_{II} for the crack problem as

$$K_{II} = \tau_0\sqrt{\pi a} \tag{3.51}$$

and the Mode I stress intensity factor $K_I = 0$. In general, the stresses in the vicinity of the right crack tip are derived as

$$\begin{aligned}
\sigma_{xx} &= -\frac{K_{II}}{\sqrt{2\pi r}} \sin\frac{1}{2}\theta \left(2 + \cos\frac{\theta}{2}\cos\frac{3\theta}{2}\right) \\
\sigma_{yy} &= \frac{K_{II}}{\sqrt{2\pi r}} \sin\frac{\theta}{2}\cos\frac{\theta}{2}\cos\frac{3}{2}\theta \\
\sigma_{xy} &= \frac{K_{II}}{\sqrt{2\pi r}} \cos\frac{1}{2}\theta \left(1 - \sin\frac{1}{2}\theta \sin\frac{3}{2}\theta\right)
\end{aligned} \tag{3.52}$$

and the near-tip displacements are

$$\begin{aligned}
u_x &= \frac{K_{II}}{8\mu\pi}\sqrt{2\pi r}\left[(2\kappa + 3)\sin\frac{\theta}{2} + \sin\frac{3\theta}{2}\right] \\
u_y &= -\frac{K_{II}}{8\mu\pi}\sqrt{2\pi r}\left[(2\kappa - 3)\cos\frac{\theta}{2} + \cos\frac{3\theta}{2}\right]
\end{aligned} \tag{3.53}$$

where the origin of the (r,θ) system has been shifted to the right crack tip.

Equation (3.52) shows that stresses also have an inverse square root singularity at the crack tip and the intensity of the singular stress field is described by the Mode II stress intensity factor. It will be seen again in Section 3.7 that the near-tip stresses Eq. (3.52) and displacements Eq. (3.53) hold for any cracked body under Mode II deformation conditions with differences only in the value of K_{II}. Hence, once the stress σ_{xy} along the crack extended line is known, the Mode II stress intensity factor can be obtained from

$$K_{II} = \lim_{r\to 0}\sqrt{2\pi r}\,\sigma_{xy}(\theta = 0) \tag{3.54}$$

The crack surface displacment may be obtained by setting $y = 0$ in Eq. (3.34) (B is ignored as it represents rigid displacements):

$$\begin{aligned}
4\mu u_x &= (\kappa + 1)\,\mathrm{Im}\hat{Z}_{II} \\
4\mu u_y &= (1 - \kappa)\,\mathrm{Re}\hat{Z}_{II}
\end{aligned}$$

Since

$$\hat{Z}_{II} = \tau_0\sqrt{z^2 - a^2}$$

we have

$$\hat{Z}_{II} = \tau_0\sqrt{x^2 - a^2} \quad \text{at } y = 0$$

The crack surfaces lie in the region $|x| < a$. Thus,

$$\hat{Z}_{II} = i\tau_0\sqrt{a^2 - x^2}$$

It is then obvious that the displacements of the upper crack surface are

$$\begin{aligned} u_y &= 0 \\ u_x &= \frac{\kappa+1}{4\mu}\tau_0\sqrt{a^2-x^2} \end{aligned} \tag{3.55}$$

The preceding expressions show that the two crack surfaces slide with each other.

3.4.3 Mode III Crack

The Mode III fracture is associated with the anti-plane deformation for which the displacements are given by

$$u_x = 0, \quad u_y = 0, \quad u_z = w(x,y) \tag{3.56}$$

The nonvanishing strains are thus given by

$$e_{xz} = \frac{1}{2}\frac{\partial w}{\partial x}, \quad e_{yz} = \frac{1}{2}\frac{\partial w}{\partial y} \tag{3.57}$$

and the corresponding stresses follow Hooke's law:

$$\sigma_{xz} = 2\mu e_{xz}, \quad \sigma_{yz} = 2\mu e_{yz} \tag{3.58}$$

The equations of equilibrium reduce to

$$\frac{\partial \sigma_{xz}}{\partial x} + \frac{\partial \sigma_{yz}}{\partial y} = 0 \tag{3.59}$$

which can be written in terms of displacement w by using Eqs. (3.57) and (3.58) as follows:

$$\nabla^2 w = 0 \tag{3.60}$$

Thus, w must be a harmonic function. Let

$$w = \frac{1}{\mu}\mathrm{Im}\{Z_{III}(z)\} \tag{3.61}$$

where $Z_{III}(z)$ is an analytic function. Substituting Eq. (3.61) in Eq. (3.57) and then Eq. (3.58), the stresses can be represented by $Z_{III}(z)$ as follows:

$$\sigma_{xz} - i\sigma_{yz} = -iZ'_{III}(z) \tag{3.62}$$

Now consider an infinite cracked body under anti-plane shear stress S shown in Figure 3.6. The boundary conditions of the crack problem are given by

$$\begin{aligned} &\sigma_{yz} = 0 \quad \text{at } |x| \le a \text{ and } y = 0 \\ &\sigma_{yz} = S \quad \text{at } |y| \to \infty \end{aligned} \tag{3.63}$$

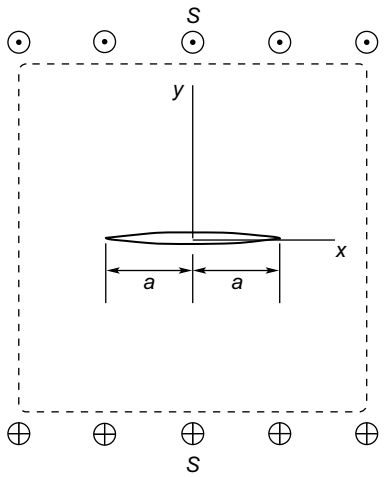

FIGURE 3.6

A crack in an infinite elastic body subjected to anti-plane shear.

Choose

$$Z_{III} = S\sqrt{z^2 - a^2} \tag{3.64}$$

We can easily show that the stresses calculated from this function satisfy the boundary conditions Eq. (3.63). Substituting Eq. (3.64) in Eq. (3.62) and using the polar coordinates defined in Eq. (3.37), the stress components can be obtained as

$$\begin{aligned} \sigma_{yz} &= \mathrm{Re}\{Z'_{III}\} = \frac{Sr}{\sqrt{r_1 r_2}} \cos\left(\theta - \frac{1}{2}\theta_1 - \frac{1}{2}\theta_2\right) \\ \sigma_{xz} &= \mathrm{Im}\{Z'_{III}\} = \frac{Sr}{\sqrt{r_1 r_2}} \sin\left(\theta - \frac{1}{2}\theta_1 - \frac{1}{2}\theta_2\right) \end{aligned} \tag{3.65}$$

Again consider the stress along the crack extended line ($\theta_1 = \theta_2 = \theta = 0$) and near the crack tip ($r_1/a \ll 1$). It is obtained from Eq. (3.65) as

$$\sigma_{yz} = \frac{S\sqrt{\pi a}}{\sqrt{2\pi r_1}}$$

Comparing these stresses with Eq. (3.1) in Section 3.1, we have the Mode III stress intensity factor K_{III} for the crack problem as

$$K_{III} = S\sqrt{\pi a} \tag{3.66}$$

In general, the near-tip stresses are obtained as

$$\begin{aligned}\sigma_{yz} &= \frac{K_{III}}{\sqrt{2\pi r_1}}\cos\frac{1}{2}\theta_1 \\ \sigma_{xz} &= -\frac{K_{III}}{\sqrt{2\pi r_1}}\sin\frac{1}{2}\theta_1\end{aligned} \tag{3.67}$$

and the anti-plane displacement is

$$w = \sqrt{\frac{2}{\pi}}\,\frac{K_{III}}{\mu}\sqrt{r_1}\,\sin\frac{1}{2}\theta_1 \tag{3.68}$$

The forms of Eqs. (3.67) and (3.68) hold for general Mode III cracks and the Mode III stress intensity factor is calculated from

$$K_{III} = \lim_{r_1\to 0}\sqrt{2\pi r_1}\,\sigma_{yz}(\theta = 0) \tag{3.69}$$

The complete displacement field is obtained using Eqs. (3.64) and (3.61) as

$$w = u_z = \frac{S}{\mu}\sqrt{r_1 r_2}\sin\frac{1}{2}(\theta_1 + \theta_2)$$

On the upper crack surface ($y = 0^+$, $|x| < a$, or $\theta_1 = \pi$, $\theta_2 = 0$), the displacement is

$$u_z = \frac{S}{\mu}\sqrt{r_1 r_2} = \frac{S}{\mu}\sqrt{a^2 - x^2} \tag{3.70}$$

3.4.4 Complex Representation of Stress Intensity Factor

Stress intensity factor is a key concept in linear elastic fracture mechanics. It will be seen in Section 3.7 that the asymptotic stress and displacement fields near a crack tip have universal forms as described in Eqs. (3.44), (3.45), (3.52), and (3.53). Solving for the stresses and displacements around a crack tip thus reduces to finding the stress intensity factors, which may be directly calculated from the solutions of the complex potential functions. It follows from the near-tip stress field Eqs. (3.44) and (3.52) that (now use (r_1,θ_1) at the crack tip $z = a$)

$$\sigma_{xx} + \sigma_{yy} = \frac{2K_I}{\sqrt{2\pi r_1}}\cos\frac{1}{2}\theta_1 \qquad \text{for Mode I}$$

$$\sigma_{xx} + \sigma_{yy} = -\frac{2K_{II}}{\sqrt{2\pi r_1}}\sin\frac{1}{2}\theta_1 \qquad \text{for Mode II}$$

For combined loading, we have

$$\sigma_{xx} + \sigma_{yy} = \frac{2K_I}{\sqrt{2\pi r_1}}\cos\frac{1}{2}\theta_1 - \frac{2K_{II}}{\sqrt{2\pi r_1}}\sin\frac{1}{2}\theta_1$$

Defining the complex stress intensity factor K,

$$K = K_I - iK_{II} \tag{3.71}$$

and recalling the definition of polar coordinates (r_1, θ_1),

$$z - a = r_1 e^{i\theta_1}$$

one can show that

$$\sigma_{xx} + \sigma_{yy} = 2\,\mathrm{Re}\left\{\frac{K}{\sqrt{2\pi(z-a)}}\right\} \quad z \to a$$

Since

$$\sigma_{xx} + \sigma_{yy} = 4\,\mathrm{Re}\{\psi'(z)\}$$

we obtain

$$\mathrm{Re}\left\{\frac{K}{\sqrt{2\pi(z-a)}}\right\} = 2\,\mathrm{Re}\{\psi'(z)\} \quad z \to a$$

The complex stress intensity factor at the crack tip $z = a$ follows from this equation:

$$K = 2\sqrt{2\pi}\lim_{z\to a}\{(\sqrt{z-a})\psi'(z)\} \tag{3.72}$$

In the last step of deriving the expression, we have used the relation

$$\mathrm{Re}\{f(z)\} = \mathrm{Re}\{g(z)\} \Rightarrow f(z) = g(z) + iC$$

where $f(z)$ and $g(z)$ are analytic functions and C is a real constant.

Proof
Let

$$h(z) = f(z) - g(z) = U_3 + iV_3$$

Thus, $h(z)$ is also analytic. Since $\mathrm{Re}\{h(z)\} = 0$, i.e.,

$$U_3 = 0$$

we have from the Cauchy-Riemann equation (3.11)

$$\frac{\partial V_3}{\partial x} = -\frac{\partial U_3}{\partial y} = 0$$

$$\frac{\partial V_3}{\partial y} = \frac{\partial U_3}{\partial x} = 0$$

Thus,

$$V_3 = \text{ real constant } = C$$

i.e.,

$$f(z) = g(z) + iC$$

If the Westergaard functions are used, we can obtain the following expression for the complex stress intensity factor at the tip $z = a$:

$$K = \sqrt{2\pi} \lim_{z \to a} \left\{ \sqrt{z - a} (Z_I - iZ_{II}) \right\} \tag{3.73}$$

For Mode III cracks, it follows from Eqs. (3.62) and (3.67) that

$$K_{III} = \sqrt{2\pi} \lim_{z \to a} \left\{ \sqrt{z - a} Z'_{III}(z) \right\} \tag{3.74}$$

3.5 FUNDAMENTAL SOLUTIONS OF STRESS INTENSITY FACTOR

In the previous section, the stress intensity factors for a crack in an infinite plane were calculated under uniform loading conditions. In engineering applications, a cracked body is generally subjected to nonuniformly distributed loads. Stress intensity factors of a cracked body under arbitrary loading conditions may be obtained using the superposition method and the fundamental solutions, which are the stress intensity factors for a cracked body subjected to concentrated forces on the crack faces.

Consider a cracked body subjected to arbitrarily loads, as shown in Figure 3.7(a). The crack surfaces are assumed in a traction free state without loss of generality. The stresses and displacements in the cracked body can be obtained by superposing the corresponding solutions of the following two problems, as shown in Figures 3.7(b) and (c). The first problem is the same elastic body without the crack subjected to the same external loads. The solutions to this first problem can be obtained using conventional methods in the theory of elasticity because no cracks are present. The second problem consists of the same cracked body subjected to the crack face tractions, which are equal only in magnitude but opposite in sign to the tractions obtained at the same crack location in the first problem.

It is evident that the superposition of the solutions of the two problems satisfies all the boundary conditions and the traction free conditions at the crack surfaces. In linear elastic fracture mechanics, the solution to the first problem is assumed

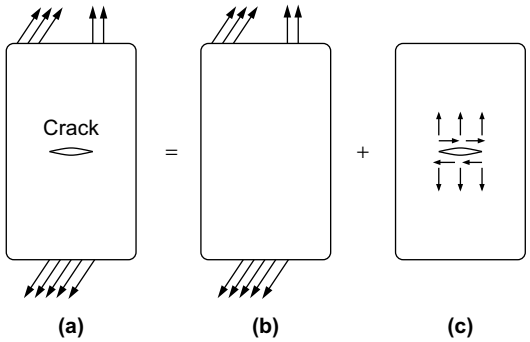

FIGURE 3.7

Superposition method of linear elastic crack problems (a) the original crack problem, (b) the first problem, (c) the second problem.

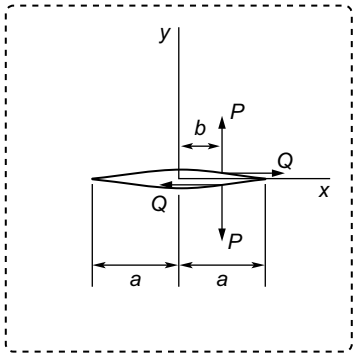

FIGURE 3.8

A crack in an infinite plate subjected to concentrated forces on the crack faces.

to be known and the stresses are finite at the location of the crack tip. The stress intensity factors therefore can be calculated from the solution to the second problem and may be obtained using the fundamental solutions. In the following sections, two fundamental solutions for a crack in an infinite plane are introduced.

3.5.1 A Finite Crack in an Infinite Plate

Consider an infinite plate containing a crack of length $2a$ subjected to a pair of compressive forces P per unit thickness at $x = b$, as shown in Figure 3.8 (the shear force Q is assumed to be absent for now). The boundary conditions of the crack problem

are formulated as follows:

$$\begin{aligned} \sigma_{yy} &= 0 \quad \text{at } |x| \le a, x \ne b \text{ and } y = 0 \\ \int_{-a}^{a} \sigma_{yy} dx &= -P \quad \text{at } y = 0^{+} \text{ and } y = 0^{-} \\ \sigma_{xy} &= 0 \quad \text{at } |x| \le a \text{ and } y = 0 \\ \sigma_{xx}, \sigma_{yy}, \sigma_{xy} &\to 0 \quad \text{at } x^2 + y^2 \to \infty \end{aligned} \tag{3.75}$$

It can be shown that the Westergaard function

$$Z_I = \frac{P}{\pi(z-b)}\sqrt{\frac{a^2-b^2}{z^2-a^2}}$$

gives the stresses that satisfy the boundary conditions Eq. (3.75). Substituting the previous function into Eq. (3.73) yields the complex stress intensity factor at the right crack tip ($z = a$):

$$\begin{aligned} K_I - iK_{II} &= \sqrt{2\pi} \lim_{z \to a} \left\{ \sqrt{z-a} \frac{P}{\pi(z-b)} \sqrt{\frac{a^2-b^2}{z^2-a^2}} \right\} \\ &= \frac{P}{\sqrt{\pi a}} \sqrt{\frac{a+b}{a-b}} \end{aligned}$$

Similarly, we can get the complex stress intensity factor at the left crack tip (note that $z - a$ in Eq. (3.73) should be replaced by $-(z+a)$ when evaluating the stress intensity factor at the tip $z = -a$). Finally, we have the stress intensity factors at the two crack tips:

$$\begin{aligned} K_I &= \frac{P}{\sqrt{\pi a}} \sqrt{\frac{a+b}{a-b}}, \quad \text{at the right crack tip } (x = a) \\ &= \frac{P}{\sqrt{\pi a}} \sqrt{\frac{a-b}{a+b}}, \quad \text{at the left crack tip } (x = -a) \end{aligned} \tag{3.76}$$

When the crack faces are subjected to a pair of shearing forces Q per unit thickness at $x = b$, as shown in Figure 3.8 (now the compressive force P is assumed absent), the Westergaard function

$$Z_{II} = \frac{Q}{\pi(z-b)}\sqrt{\frac{a^2-b^2}{z^2-a^2}}$$

gives the stresses that satisfy the following boundary conditions of the Mode II crack problem, that is,

$$\begin{aligned} \sigma_{xy} &= 0 \quad \text{at } |x| \le a, x \ne b \text{ and } y = 0 \\ \int_{-a}^{a} \sigma_{xy} dx &= -Q \quad \text{at } y = 0^+ \text{ and } y = 0^- \\ \sigma_{yy} &= 0 \quad \text{at } |x| \le a \text{ and } y = 0 \\ \sigma_{xx}, \sigma_{yy}, \sigma_{xy} &\to 0 \quad \text{at } x^2 + y^2 \to \infty \end{aligned} \tag{3.77}$$

Substituting the Westergaard function into Eq. (3.73), we have the Mode II stress intensity factors:

$$\begin{aligned} K_{II} &= \frac{Q}{\sqrt{\pi a}} \sqrt{\frac{a+b}{a-b}}, \quad \text{at the right crack tip } (x = a) \\ &= \frac{Q}{\sqrt{\pi a}} \sqrt{\frac{a-b}{a+b}}, \quad \text{at the left crack tip } (x = -a) \end{aligned} \tag{3.78}$$

3.5.2 Stress Intensity Factors for a Crack Subjected to Arbitrary Crack Face Loads

In linear elastcity, it has been known that the stress (and displacement) in an elastic body subjected to a number of external loads is the sum of the stresses corresponding to each individual load. This is the so-called superposition principle of linear elastic systems. We now apply this principle to problems of cracks in linear elastic solids. The fundamental solutions Eqs. (3.76) and (3.78) can thus be used to obtain stress intensity factors under arbitrary crack face loads.

Consider a crack of length $2a$ in an infinite plate subjected to arbitrarily distributed pressure $p(x)$ on the crack faces. To obtain the stress intensity factor, we consider an infinitesimal length element $d\xi$ at $x = \xi$ on the crack face. The force exerted on this length element is $p(\xi)d\xi$, which induces the following stress intensity factors according to the fundamental solution Eq. (3.76):

$$\begin{aligned} dK_I &= \frac{p(\xi)d\xi}{\sqrt{\pi a}} \sqrt{\frac{a+\xi}{a-\xi}}, \quad \text{at the right crack tip } (x = a) \\ &= \frac{p(\xi)d\xi}{\sqrt{\pi a}} \sqrt{\frac{a-\xi}{a+\xi}}, \quad \text{at the left crack tip } (x = -a) \end{aligned}$$

The total stress intensity factors due to the distributed pressure can be obtained by integrating the preceding expression along the crack face (from $\xi = -a$ to a).

We have

$$K_I = \frac{1}{\sqrt{\pi a}} \int_{-a}^{a} p(\xi) \sqrt{\frac{a+\xi}{a-\xi}} d\xi, \quad \text{at the right crack tip } (x = a)$$

$$= \frac{1}{\sqrt{\pi a}} \int_{-a}^{a} p(\xi) \sqrt{\frac{a-\xi}{a+\xi}} d\xi, \quad \text{at the left crack tip } (x = -a) \tag{3.79}$$

Similarly, the Mode II stress intensity factors corresponding to the distributed shearing traction $q(x)$ on the crack surfaces can be obtained by using the fundamental solution Eq. (3.78) as follows:

$$K_{II} = \frac{1}{\sqrt{\pi a}} \int_{-a}^{a} q(\xi) \sqrt{\frac{a+\xi}{a-\xi}} d\xi, \quad \text{at the right crack tip } (x = a)$$

$$= \frac{1}{\sqrt{\pi a}} \int_{-a}^{a} q(\xi) \sqrt{\frac{a-\xi}{a+\xi}} d\xi, \quad \text{at the left crack tip } (x = -a) \tag{3.80}$$

3.5.3 A Semi-infinite Crack in an Infinite Medium

Consider an infinite medium containing a semi-infinite crack subjected to a pair of compressive forces P per unit thickness, as shown in Figure 3.9. The boundary

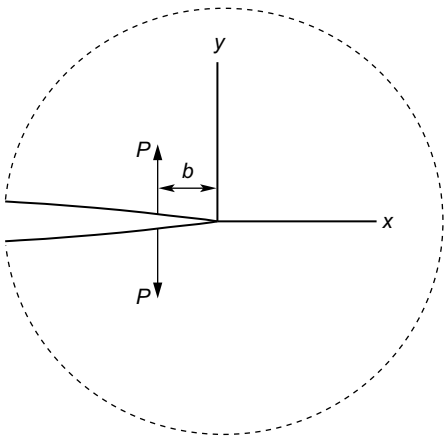

FIGURE 3.9

A semi-infinite crack in an infinite plate subjected to concentrated forces on the crack faces.

conditions of the crack problem are

$$\sigma_{yy} = 0 \quad \text{at } -\infty < x < 0,\ x \neq -b \text{ and } y = 0$$

$$\int_{-\infty}^{0} \sigma_{yy} dx = -P \quad \text{at } y = 0^{+} \text{ and } y = 0^{-}$$

$$\sigma_{xy} = 0 \quad \text{at } -\infty < x < 0 \text{ and } y = 0$$

$$\sigma_{xx}, \sigma_{yy}, \sigma_{xy} \to 0 \quad \text{at } x^2 + y^2 \to \infty$$

The Westergaard function for the semi-infinite crack problem is given by

$$Z_I = \frac{P}{\pi(z+b)}\sqrt{\frac{b}{z}}$$

Substituting the function here into Eq. (3.73), we have the Mode I stress intensity factor at the crack tip ($z = 0$):

$$K_I = \sqrt{2\pi} \lim_{z \to 0} \left\{ \sqrt{z} \frac{P}{\pi(z+b)} \sqrt{\frac{b}{z}} \right\}$$

$$= P\sqrt{\frac{2}{\pi b}} \tag{3.81}$$

3.6 FINITE SPECIMEN SIZE EFFECTS

In Sections 3.4 and 3.5, we have introduced stress intensity factor solutions for some basic crack problems of infinite media. These solutions may be used when the crack length is much smaller than the in-plane size of the cracked body. When the crack length is of the order of the size of the cracked body, the stress intensity factor will be influenced by the size of the cracked body. In general, numerical methods (for example, the finite element method) are used to calculate stress intensity factors for cracks in finite size media.

Now consider a center-cracked plate subjected to tension as shown in Figure 3.10. The height and width of the plate are $2H$ and $2b$, respectively. The crack length is $2a$. The general form of the stress intensity factor may be expressed as

$$K_I = \sigma\sqrt{\pi a} F(a/b, a/H) \tag{3.82}$$

where $F(a/b, a/H)$ is a dimensionless function of a/b and a/H. When $H >> b$, the plate may be regarded as an infinite strip. In this case, the parameter a/H may be dropped in $F(a/b, a/H)$ in Eq. (3.82) and some empirical expressions for $F(a/b)$

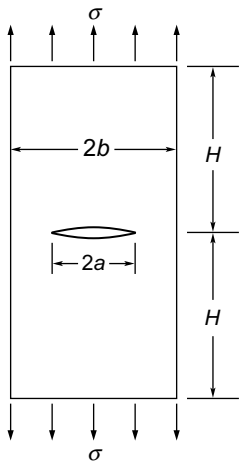

FIGURE 3.10

A finite plate with a center crack subjected to tension.

were proposed by curve-fitting the numerical result of the stress intensity factor. For example, Irwin [3-1] proposed the following approximate formula:

$$F(a/b) = 1 + 0.128\left(\frac{a}{b}\right) - 0.288\left(\frac{a}{b}\right)^2 + 1.525\left(\frac{a}{b}\right)^3 \tag{3.83}$$

The relative error between this formula here and that of the numerical solution is less that 0.5% when $a/b \leq 0.7$. It is noted that the preceding stress intensity factor for the center-cracked plate reduces to that for an infinite plate ($\sigma\sqrt{\pi a}$) when $a/b \to 0$.

The Appendix lists stress intensity factor solutions for some typical cracked specimens.

3.7 WILLIAMS' CRACK TIP FIELDS

In the previous sections, explicit stress and displacement fields near the crack tip were obtained using the Westergaard function method. One common characteristic feature of these solutions is that the stresses have an inverse square root singularity at the crack tip and the unambiguous functional forms of these near-tip stress and displacement fields do not depend on the applied load and the geometry of the cracked body. For instance, the near-tip stress and displacement fields for a crack in an infinite plate subjected to remote loading are exactly the same as those for the cracked plate subjected to crack face concentrated loading. This observation regarding the unique functional form for the near-tip fields can be verified using the eigenfunction expansion method for any crack geometries and loading conditions presented by Williams [3-5, 3-6].

3.7.1 Williams' Crack Tip Stress and Displacement Fields: Mode I and II

It has been shown in Section 3.2 that stresses and displacements can be repesented by the Airy stress function ϕ, which satisfies the following biharmonic equation:

$$\nabla^2\nabla^2\phi = 0 \tag{3.84}$$

where the Laplacian operator ∇^2 in the polar coordinate system (r,θ) centered at the crack tip (see Figure 3.11) is given by

$$\nabla^2 = \frac{\partial^2}{\partial r^2} + \frac{1}{r}\frac{\partial}{\partial r} + \frac{1}{r^2}\frac{\partial^2}{\partial \theta^2}$$

The Airy stress function near the crack tip may be expanded into the following series:

$$\phi = \sum_{n=0}^{\infty} r^{\lambda_n+1} F_n(\theta) \tag{3.85}$$

where λ_n are eigenvalues to be determined and $F_n(\theta)$ are the corresponding eigenfunctions. Substitution of Eq. (3.85) in Eq. (3.84) yields

$$\frac{d^4F_n(\theta)}{d\theta^4} + 2(\lambda_n^2+1)\frac{d^2F_n(\theta)}{d\theta^2} + (\lambda_n^2-1)^2F_n(\theta) = 0$$

The solution of this equation for $F_n(\theta)$ has the following form:

$$\begin{aligned} F_n(\theta) = {} & A_n \sin(\lambda_n+1)\theta + B_n\cos(\lambda_n+1)\theta \\ & + C_n\sin(\lambda_n-1)\theta + D_n\cos(\lambda_n-1)\theta \end{aligned} \tag{3.86}$$

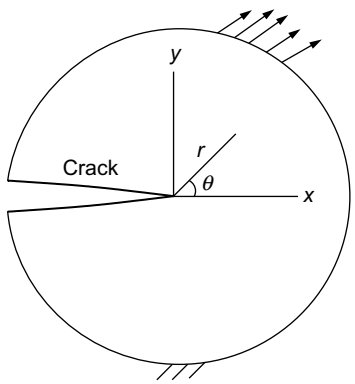

FIGURE 3.11

A cracked plate and the coordinate systems.

where A_n, B_n, C_n, and D_n are unknown constants. The stresses need to satisfy the following traction free boundary conditions along the crack surfaces:

$$\sigma_{\theta\theta} = \sigma_{r\theta} = 0, \quad \theta = \pm\pi \tag{3.87}$$

Mode I Case

For Mode I crack problems, the Airy stress function is an even function of θ. The constants A_n and C_n in Eq. (3.86) become zero and the Airy function can be written as

$$\phi = \sum_{n=0}^{\infty} r^{\lambda_n+1} \left[B_n \cos(\lambda_n + 1)\theta + D_n \cos(\lambda_n - 1)\theta\right] \tag{3.88}$$

The stresses in the polar coordinate system can be obtained from the Airy function as follows:

$$\begin{aligned}
\sigma_{rr} &= \frac{1}{r^2}\frac{\partial^2\phi}{\partial\theta^2} + \frac{1}{r}\frac{\partial\phi}{\partial r} = \sum_{n=0}^{\infty} r^{\lambda_n-1}\left[F_n''(\theta) + (\lambda_n + 1)F_n(\theta)\right] \\
&= -\sum_{n=0}^{\infty} \lambda_n r^{\lambda_n-1}\left[B_n(\lambda_n + 1)\cos(\lambda_n + 1)\theta + D_n(\lambda_n - 3)\cos(\lambda_n - 1)\theta\right] \\
\sigma_{\theta\theta} &= \frac{\partial^2\phi}{\partial r^2} = \sum_{n=0}^{\infty} r^{\lambda_n-1}\lambda_n(\lambda_n + 1)F_n(\theta) \\
&= \sum_{n=0}^{\infty} r^{\lambda_n-1}\lambda_n(\lambda_n + 1)\left[B_n\cos(\lambda_n + 1)\theta + D_n\cos(\lambda_n - 1)\theta\right] \\
\sigma_{r\theta} &= -\frac{\partial}{\partial r}\left(\frac{1}{r}\frac{\partial\phi}{\partial\theta}\right) = -\sum_{n=0}^{\infty} \lambda_n r^{\lambda_n-1}F_n'(\theta) \\
&= \sum_{n=0}^{\infty} \lambda_n r^{\lambda_n-1}\left[B_n(\lambda_n + 1)\sin(\lambda_n + 1)\theta + D_n(\lambda_n - 1)\sin(\lambda_n - 1)\theta\right]
\end{aligned} \tag{3.89}$$

The displacements in the polar coordinate system may be obtained using Hooke's law and the strain-displacement relations given as:

$$\begin{aligned}
\frac{\partial u_r}{\partial r} &= e_{rr} = \frac{1}{2\mu}\left[\sigma_{rr} - \frac{3-\kappa}{4}(\sigma_{rr} + \sigma_{\theta\theta})\right] \\
\frac{u_r}{r} + \frac{1}{r}\frac{\partial u_\theta}{\partial\theta} &= e_{\theta\theta} = \frac{1}{2\mu}\left[\sigma_{\theta\theta} - \frac{3-\kappa}{4}(\sigma_{rr} + \sigma_{\theta\theta})\right] \\
\frac{1}{r}\frac{\partial u_r}{\partial\theta} + r\frac{\partial}{\partial r}\left(\frac{u_\theta}{r}\right) &= e_{r\theta} = \frac{1}{2\mu}\sigma_{r\theta}
\end{aligned} \tag{3.90}$$

where

$$\kappa = \begin{cases} 3-4\nu & \text{for plane strain} \\ \dfrac{3-\nu}{1+\nu} & \text{for plane stress} \end{cases}$$

Substituting the stresses Eq. (3.89) in Eq. (3.90) and performing appropriate integration gives the following series form solutions for the displacements:

$$\begin{aligned} u_r &= \frac{1}{2\mu}\sum_{n=0}^{\infty} r^{\lambda_n}\{-(\lambda_n+1)F_n(\theta) + (1+\kappa)D_n\cos(\lambda_n-1)\theta\} \\ u_\theta &= \frac{1}{2\mu}\sum_{n=0}^{\infty} r^{\lambda_n}\{-F_n'(\theta) + (1+\kappa)D_n\sin(\lambda_n-1)\theta\} \end{aligned} \tag{3.91}$$

Substituting the stresses Eq. (3.89) in the boundary conditions Eq. (3.87) leads to the following two simultaneous equations for the constants B_n and D_n:

$$\begin{aligned} B_n\cos(\lambda_n+1)\pi + D_n\cos(\lambda_n-1)\pi &= 0 \\ B_n(\lambda_n+1)\sin(\lambda_n+1)\pi + D_n(\lambda_n-1)\sin(\lambda_n-1)\pi &= 0 \end{aligned} \tag{3.92}$$

The existence of nontrivial solutions for B_n and D_n for the system of homogeneous equations leads to the following characteristic equation of the eigenvalue λ_n:

$$\sin(2\lambda_n\pi) = 0 \tag{3.93}$$

The roots of this equation are

$$\lambda_n = \frac{n}{2}, \quad n = 0, \pm 1, \pm 2, \ldots$$

It follows from the displacement expression Eq. (3.91) that the negative values of λ_n would give rise to infinite displacements at the crack tip $r = 0$, which is not physically permissible, and hence should be excluded. A zero λ_n ($n = 0$) leads to physically impermissible unbounded strain energy in a small disc area around the crack tip and should also be excluded. Hence, only positive eigenvalues are kept. Thus,

$$\lambda_n = \frac{n}{2}, \quad n = 1, 2, \ldots \tag{3.94}$$

Substituting the eigenvalues above in Eq. (3.92), we obtain the following relation between B_n and D_n:

$$\begin{aligned} B_n &= -\frac{(\frac{n}{2}-1)\sin(\frac{n}{2}-1)\pi}{(\frac{n}{2}+1)\sin(\frac{n}{2}+1)\pi}D_n = -\frac{n-2}{n+2}D_n, \quad n = 1,3,5,\ldots \\ B_n &= -\frac{\cos\left(\frac{n}{2}-1\right)\pi}{\cos\left(\frac{n}{2}+1\right)\pi}D_n = -D_n, \quad n = 2,4,6,\ldots \end{aligned} \tag{3.95}$$

The constants D_n depend on the loading and boundary conditions of the specific crack problem as only the traction-free conditions on the crack faces are used in deriving the crack tip asymptotic solutions. Substituting the eigenvalues Eq. (3.94) in Eq. (3.89), we obtain the following series form solution for Mode I stresses near the crack tip:

$$\begin{aligned}
\sigma_{rr} &= -\sum_{n=1}^{\infty} r^{\frac{n}{2}-1}\left(\frac{n}{2}\right)\left[B_n\left(\frac{n}{2}+1\right)\cos\left(\frac{n}{2}+1\right)\theta + D_n\left(\frac{n}{2}-3\right)\cos\left(\frac{n}{2}-1\right)\theta\right] \\
\sigma_{\theta\theta} &= \sum_{n=1}^{\infty} r^{\frac{n}{2}-1}\left(\frac{n}{2}\right)\left(\frac{n}{2}+1\right)\left[B_n\cos\left(\frac{n}{2}+1\right)\theta + D_n\cos\left(\frac{n}{2}-1\right)\theta\right] \\
\sigma_{r\theta} &= \sum_{n=1}^{\infty} r^{\frac{n}{2}-1}\left(\frac{n}{2}\right)\left[B_n\left(\frac{n}{2}+1\right)\sin\left(\frac{n}{2}+1\right)\theta + D_n\left(\frac{n}{2}-1\right)\sin\left(\frac{n}{2}-1\right)\theta\right]
\end{aligned} \tag{3.96}$$

where B_n and D_n satisfy relation Eq. (3.95).

The first two terms ($n = 1, 2$) in the series solution just shown are given by

$$\begin{aligned}
\sigma_{rr} &= D_1 r^{-1/2}\left[-\frac{1}{4}\cos\frac{3\theta}{2} + \frac{5}{4}\cos\frac{\theta}{2}\right] + 2D_2\cos 2\theta + 2D_2 + O\left(r^{1/2}\right) \\
\sigma_{\theta\theta} &= D_1 r^{-1/2}\left[\frac{1}{4}\cos\frac{3\theta}{2} + \frac{3}{4}\cos\frac{\theta}{2}\right] - 2D_2\cos 2\theta + 2D_2 + O\left(r^{1/2}\right) \\
\sigma_{r\theta} &= D_1 r^{-1/2}\left[\frac{1}{4}\sin\frac{3\theta}{2} + \frac{1}{4}\sin\frac{\theta}{2}\right] - 2D_2\sin 2\theta + O\left(r^{1/2}\right)
\end{aligned} \tag{3.97}$$

Clearly only the first terms ($n = 1$) are singular at the crack tip. With the definition of Mode I stress intensity factor,

$$K_I = \lim_{r\to 0}\sqrt{2\pi r}\,\sigma_{\theta\theta}(r, 0)$$

the constant D_1 in the first terms is related to K_I as follows:

$$D_1 = \frac{K_I}{\sqrt{2\pi}} \tag{3.98}$$

The constant D_2 in the second terms is related to the so-called T-stress. The rectangular stress components corresponding to the stresses in Eq. (3.97) are

$$\begin{aligned}
\sigma_{xx} &= D_1 r^{-1/2}\cos\frac{1}{2}\theta\left(1 - \sin\frac{1}{2}\theta\sin\frac{3}{2}\theta\right) + T + O\left(r^{1/2}\right) \\
\sigma_{yy} &= D_1 r^{-1/2}\cos\frac{1}{2}\theta\left(1 + \sin\frac{1}{2}\theta\sin\frac{3}{2}\theta\right) + O\left(r^{1/2}\right) \\
\sigma_{xy} &= D_1 r^{-1/2}\sin\frac{1}{2}\theta\cos\frac{1}{2}\theta\cos\frac{3}{2}\theta + O\left(r^{1/2}\right)
\end{aligned} \tag{3.99}$$

where $T = 4D_2$ is the T-stress, the constant term in the σ_{xx} expansion. It has been shown that the T-stress significantly influences the shape and size of the plastic zone around the crack tip [3-7].

It is noted that the first three terms in the expansion of the opening stress ahead of the crack tip ($x > 0,\ y = 0$) are

$$\sigma_{yy} = \frac{K_I}{\sqrt{2\pi x}} + b_0 x^{1/2} + b_1 x^{3/2}$$

It is clear that there is no equivalent T-stress (constant stress term) in the crack opening stress expansion.

Mode II Case

For Mode II crack problems, the Airy stress function is an odd function of θ. The constants B_n and D_n in Eq. (3.86) become zero and the Airy function can be written as

$$\phi = \sum_{n=0}^{\infty} r^{\lambda_n+1} [A_n \sin(\lambda_n + 1)\theta + C_n \sin(\lambda_n - 1)\theta] \tag{3.100}$$

The stresses in the polar coordinate system can be obtained from the Airy function as follows:

$$\begin{aligned}
\sigma_{rr} &= -\sum_{n=0}^{\infty} \lambda_n r^{\lambda_n-1} [A_n(\lambda_n + 1)\sin(\lambda_n + 1)\theta + C_n(\lambda_n - 3)\sin(\lambda_n - 1)\theta] \\
\sigma_{\theta\theta} &= \sum_{n=0}^{\infty} r^{\lambda_n-1} \lambda_n (\lambda_n + 1) [A_n \sin(\lambda_n + 1)\theta + C_n \sin(\lambda_n - 1)\theta] \\
\sigma_{r\theta} &= -\sum_{n=0}^{\infty} \lambda_n r^{\lambda_n-1} [A_n(\lambda_n + 1)\cos(\lambda_n + 1)\theta + C_n(\lambda_n - 1)\cos(\lambda_n - 1)\theta]
\end{aligned} \tag{3.101}$$

The displacements in the polar coordinate system are given by

$$\begin{aligned}
u_r &= \frac{1}{2\mu} \sum_{n=0}^{\infty} r^{\lambda_n} \{-(\lambda_n + 1)F_n(\theta) + (1 + \kappa)C_n \sin(\lambda_n - 1)\theta\} \\
u_\theta &= \frac{1}{2\mu} \sum_{n=0}^{\infty} r^{\lambda_n} \{-F_n'(\theta) - (1 + \kappa)C_n \cos(\lambda_n - 1)\theta\}
\end{aligned} \tag{3.102}$$

Substiting the stresses Eq. (3.101) into the boundary conditions Eq. (3.87) leads to the following two simultaneous equations for the constants A_n and C_n:

$$\begin{aligned}
A_n \sin(\lambda_n + 1)\pi + C_n \sin(\lambda_n - 1)\pi &= 0 \\
A_n(\lambda_n + 1)\cos(\lambda_n + 1)\pi + C_n(\lambda_n - 1)\cos(\lambda_n - 1)\pi &= 0
\end{aligned} \tag{3.103}$$

The existence of nontrivial solutions for A_n and C_n for the system of homogeneous equations here leads to the same characteristic equation (3.93). Hence, the eigenvalues λ_n are the same as those for Mode I in Eq. (3.94). Substituting the eigenvalues in Eq. (3.103) yields the following relation between A_n and C_n:

$$\begin{aligned} A_n &= -\frac{\sin\left(\frac{n}{2}-1\right)\pi}{\sin\left(\frac{n}{2}+1\right)\pi}C_n = -C_n, \quad n = 1,3,5,... \\ A_n &= -\frac{\left(\frac{n}{2}-1\right)\cos\left(\frac{n}{2}-1\right)\pi}{\left(\frac{n}{2}+1\right)\cos\left(\frac{n}{2}+1\right)\pi}C_n = -\frac{n-2}{n+2}C_n, \quad n = 2,4,6,... \end{aligned} \tag{3.104}$$

Again, the constants C_n need to be determined using the loading and boundary conditions of the specific crack problem. Substitution of the eigenvalues Eq. (3.94) in Eq. (3.101) yields the following series form solution for Mode II stresses near the crack tip:

$$\begin{aligned} \sigma_{rr} &= -\sum_{n=1}^{\infty} r^{\frac{n}{2}-1}\left(\frac{n}{2}\right)\left[A_n\left(\frac{n}{2}+1\right)\sin\left(\frac{n}{2}+1\right)\theta + C_n\left(\frac{n}{2}-3\right)\sin\left(\frac{n}{2}-1\right)\theta\right] \\ \sigma_{\theta\theta} &= \sum_{n=1}^{\infty} r^{\frac{n}{2}-1}\left(\frac{n}{2}\right)\left(\frac{n}{2}+1\right)\left[A_n\sin\left(\frac{n}{2}+1\right)\theta + C_n\sin\left(\frac{n}{2}-1\right)\theta\right] \\ \sigma_{r\theta} &= -\sum_{n=1}^{\infty} r^{\frac{n}{2}-1}\left(\frac{n}{2}\right)\left[A_n\left(\frac{n}{2}+1\right)\cos\left(\frac{n}{2}+1\right)\theta + C_n\left(\frac{n}{2}-1\right)\cos\left(\frac{n}{2}-1\right)\theta\right] \end{aligned} \tag{3.105}$$

where A_n and C_n satisfy the relation Eq. (3.104). Again, only the first terms ($n = 1$) in this series solution are singular at the crack tip and they are given by

$$\begin{aligned} \sigma_{rr} &= C_1 r^{-1/2}\left[\frac{3}{4}\sin\frac{3\theta}{2} - \frac{5}{4}\sin\frac{\theta}{2}\right] \\ \sigma_{\theta\theta} &= C_1 r^{-1/2}\left[-\frac{3}{4}\sin\frac{3\theta}{2} - \frac{3}{4}\sin\frac{\theta}{2}\right] \\ \sigma_{r\theta} &= C_1 r^{-1/2}\left[\frac{3}{4}\cos\frac{3\theta}{2} + \frac{1}{4}\cos\frac{\theta}{2}\right] \end{aligned} \tag{3.106}$$

Using the definition of Mode II stress intensity factor,

$$K_{II} = \lim_{r\to 0}\sqrt{2\pi r}\,\sigma_{r\theta}(r,0)$$

the constant C_1 in the preceding equations can be related to K_{II} as follows:

$$C_1 = \frac{K_{II}}{\sqrt{2\pi}} \tag{3.107}$$

For combined Mode I and II crack problems, the stresses are the superpostion of Eq. (3.96) for Mode I and Eq. (3.105) for Mode II. The first terms in the stress solutions, when transformed to the Cartesian components, have the same form as those in Eqs. (3.44) and (3.52) in Section 3.4 for the specific crack problems considered.

3.7.2 Williams' Crack Tip Stress and Displacement Fields: Mode III

The asymptotic series expansion method introduced for Mode I and Mode II cracks may also be used to obtain the crack tip fields for Mode III cracks. Corresponding to the basic equations (3.57), (3.58), and (3.59) in the Cartesian coordinates, the basic equations in the polar coordinates are given as follows:

$$e_{rz} = \frac{1}{2}\frac{\partial w}{\partial r}, \quad e_{\theta z} = \frac{1}{2r}\frac{\partial w}{\partial \theta} \tag{3.108}$$

$$\sigma_{rz} = 2\mu e_{rz}, \quad \sigma_{\theta z} = 2\mu e_{\theta z} \tag{3.109}$$

$$\frac{\partial \sigma_{rz}}{\partial r} + \frac{1}{r}\frac{\partial \sigma_{\theta z}}{\partial \theta} + \frac{\sigma_{rz}}{r} = 0 \tag{3.110}$$

The anti-plane displacement $w = w(r,\theta)$ satisfies the harmonic equation

$$\nabla^2 w = 0 \tag{3.111}$$

where ∇^2 in polar coordinates is given by

$$\nabla^2 = \frac{1}{r}\frac{\partial}{\partial r}\left(r\,\frac{\partial}{\partial r}\right) + \frac{1}{r^2}\frac{\partial^2}{\partial \theta^2}$$

The traction-free condition on the crack surfaces and the antisymmetry condition along the crack extended line lead to the boundary conditions:

$$\begin{aligned} \sigma_{\theta z} &= 0 \quad \text{at } \theta = \pm\pi,\ r > 0 \\ w &= 0 \quad \text{at } \theta = 0,\ r > 0 \end{aligned} \tag{3.112}$$

By the separation of variables approach, we assume the following expansion of displacement w near the crack tip ($r = 0$):

$$w(r,\theta) = \sum_{n=0}^{\infty} r^{\lambda_n} f_n(\theta) \tag{3.113}$$

where $f_n(\theta)$ are the eigenfunctions and λ_n are the eigenvalues to be determined. Substitution of Eq. (3.113) in Eq. (3.111) yields

$$\sum_{n=0}^{\infty} r^{\lambda_n - 2}\left(\lambda_n^2 f_n + f_n''\right) = 0$$

which leads to

$$f_n'' + \lambda_n^2 f_n = 0$$

The general solution for the preceding ordinary differential equation is readily obtained as

$$f_n(\theta) = A_n \cos\lambda_n\theta + B_n \sin\lambda_n\theta$$

Thus,

$$\begin{aligned} w(r,\theta) &= \sum_{n=0}^{\infty} r^{\lambda_n} (A_n \cos\lambda_n\theta + B_n \sin\lambda_n\theta) \\ \sigma_{rz} &= \mu \sum_{n=0}^{\infty} \lambda_n r^{\lambda_n - 1} (A_n \cos\lambda_n\theta + B_n \sin\lambda_n\theta) \\ \sigma_{\theta z} &= \mu \sum_{n=0}^{\infty} \lambda_n r^{\lambda_n - 1} (-A_n \sin\lambda_n\theta + B_n \cos\lambda_n\theta) \end{aligned} \tag{3.114}$$

Substitition of Eq. (3.114) in the boundary conditions Eq. (3.112) gives

$$\begin{aligned} -A_n \sin\lambda_n\pi + B_n \cos\lambda_n\pi &= 0 \\ A_n &= 0 \end{aligned}$$

For a nontrivial solution (B_n cannot be zero) for the previous homogeneous equations, we require

$$\cos\lambda_n\pi = 0$$

which yields

$$\lambda_n = n - \frac{1}{2}, \quad n = 1,2,3,...$$

The negative eigenvalues have been excluded to avoid unbounded displacement at $r = 0$. Substituting this eigenvalues into Eq. (3.114) yields

$$\begin{aligned} w(r,\theta) &= \sum_{n=1}^{\infty} B_n r^{n-\frac{1}{2}} \sin\left(n - \frac{1}{2}\right)\theta \\ \sigma_{rz} &= \mu \sum_{n=1}^{\infty} \left(n - \frac{1}{2}\right) B_n r^{n-\frac{3}{2}} \sin\left(n - \frac{1}{2}\right)\theta \\ \sigma_{\theta z} &= \mu \sum_{n=1}^{\infty} \left(n - \frac{1}{2}\right) B_n r^{n-\frac{3}{2}} \cos\left(n - \frac{1}{2}\right)\theta \end{aligned} \tag{3.115}$$

It is obvious from these expansions that only the first term ($n = 1$) produces singular stresses in the form

$$\sigma_{rz} = B_1 \frac{\mu}{2}\, r^{-\frac{1}{2}} \sin\frac{\theta}{2}$$
$$\sigma_{\theta z} = B_1 \frac{\mu}{2}\, r^{-\frac{1}{2}} \cos\frac{\theta}{2}$$

and the corresponding displacement is

$$w = B_1 r^{\frac{1}{2}} \sin\frac{\theta}{2}$$

At $\theta = 0$,

$$\sigma_{yz} = \sigma_{\theta z} = \frac{B_1 \mu}{2\sqrt{r}}$$

Thus, B_1 is related to the Mode III stress intensity factor K_{III} by

$$K_{III} = \sqrt{\frac{\pi}{2}}\, \mu B_1$$

and the near-tip stress and displacement field can be expressed in the form

$$\sigma_{rz} = \frac{K_{III}}{\sqrt{2\pi r}} \sin\frac{\theta}{2}$$
$$\sigma_{\theta z} = \frac{K_{III}}{\sqrt{2\pi r}} \cos\frac{\theta}{2}$$
$$w = \frac{K_{III}}{\pi\mu}\sqrt{2\pi r} \sin\frac{\theta}{2}$$

The stress components in the Cartesian coordinate system are

$$\sigma_{xz} = -\frac{K_{III}}{\sqrt{2\pi r}} \sin\frac{\theta}{2}$$
$$\sigma_{yz} = \frac{K_{III}}{\sqrt{2\pi r}} \cos\frac{\theta}{2}$$
$$w = \frac{K_{III}}{\pi\mu}\sqrt{2\pi r} \sin\frac{\theta}{2}$$

which are identical to Eqs. (3.67) and (3.68).

3.8 *K*-DOMINANCE

It is now clear that the stress field near a crack tip consists of two parts, one is singular at the crack tip and the other is nonsigular. The singular part becomes dominant if the location of interest approaches sufficiently close to the crack tip. In that case, the near-tip stress field can be effectively described by the singular stress field or, equivalently, by the stress intensity factor. This feature is of fundamental importance and is the foundation of the stress intensity factor-based fracture criterion of Irwin [3-1]. The successful use of the stress intensity factor to predict crack growth (fracture) depends on whether the singular stress term alone can represent the state of stress in the "fracture process zone," a region ahead of the crack tip in which the material failure process initiates. The knowledge of the *K*-dominance zone size is thus pertinent to the proper understanding and applicability of the fracture criterion.

To study the *K*-dominance zone size, the nonsingular part of the stress field is needed. For Mode I cracks, the normal stress σ_{yy} along the crack line ($x > 0$, $y = 0$) plays an essential role in crack extension. We define the degree of *K*-dominance at a point along the x-axis as

$$\Lambda = \frac{K_I/\sqrt{2\pi x}}{K_I/\sqrt{2\pi x} + \left|\text{nonsingular part of } \sigma_{yy}\right|} \tag{3.116}$$

where σ_{yy} is the total stress. Note that the absolute value of the nonsingular part of the normal stress is taken to ensure that the value of Λ does not exceed unity. A value of Λ close to unity means that the singular stress is dominant.

First consider a crack of length $2a$ in an infinite plate subjected to biaxial tension σ_0 as shown in Figure 3.3. The complete solution is available for this problem. From Eq. (3.41), the opening stress σ_{yy} along the extended crack line can be written as (now $x = 0$ is at the right crack tip)

$$\sigma_{yy} = \frac{(x+a)\sigma_0}{\sqrt{x(x+2a)}}, \quad x > 0$$

Since σ_{yy} is positive, the degree of *K*-dominance according to Eq. (3.116) is

$$\Lambda = \frac{K_I/\sqrt{2\pi x}}{\sigma_{yy}} = \frac{\sqrt{2+x/a}}{\sqrt{2}(1+x/a)}$$

The *K*-dominance zone size x_K for $\Lambda = 0.95$ can be determined from this equation with the result

$$x_K \approx 0.07a$$

The previous result indicates that, for a central crack in an infinite plate subjected to uniform biaxial tension, the singular stress consititutes at least 95% of the opening stress within the range $x \le x_K$.

Next, consider the example of a finite rectangular plate containing a center crack subjected to a uniform tensile stress as shown in Figure 3.12. The normal stress σ_{yy} along the crack line ($x > 0$, $y = 0$) is calculated using the finite element method with $W/a = 2$. Figure 3.13 shows the normalized normal stress distributions $\sigma_{yy}\sqrt{2\pi x}/K_0$ for three plates of different heights, where $K_0 = \sigma_0\sqrt{\pi a}$. It is noted that, if the singular stress is dominant near the crack tip, the plot should be nearly a straight line in the

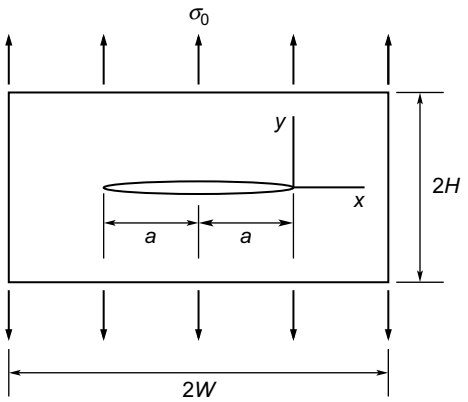

FIGURE 3.12

A cracked rectangular plate subjected to uniform tension.

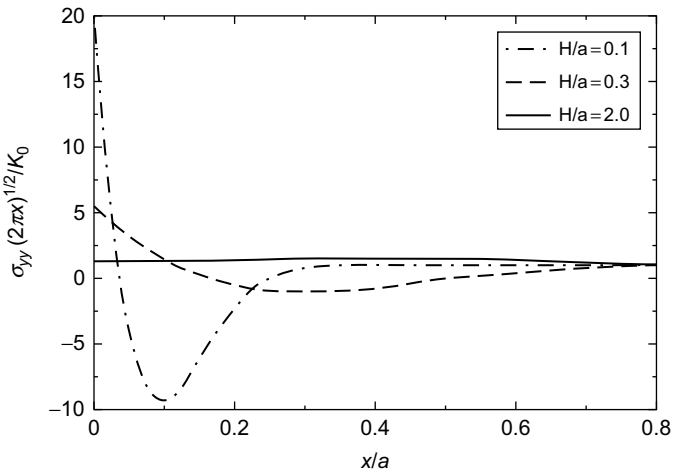

FIGURE 3.13

Normalized normal stress, $\sigma_{yy}\sqrt{2\pi x}/K_0$, along the crack line.

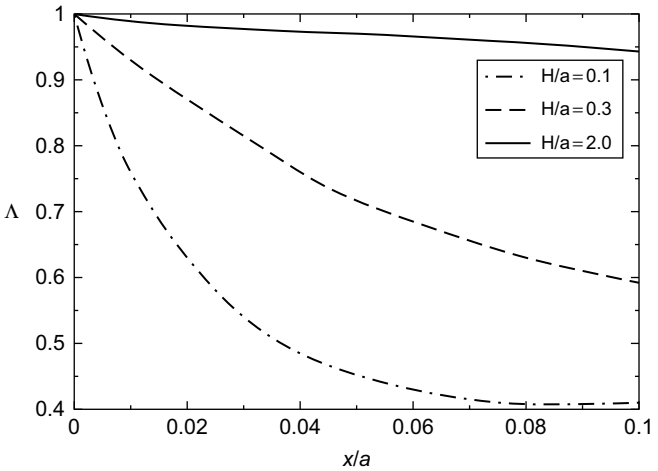

FIGURE 3.14

The degree of K-dominance, Λ, along the crack line.

crack tip region as in the case of $H/a = 2$. Figure 3.14 shows the plots of the degree of K-dominance, Λ, along the x-axis for the three cases.

The results in Figures 3.13 and 3.14 clearly show that, as the height of the plate decreases, the size of the K-dominance region also decreases. For $H/a = 0.1$ and $\Lambda = 0.95$, the size of the K-dominance zone can be estimated from Figure 3.14 to be $x_K \approx 0.002a$. In other words, the region in which the singular stress is dominant is very small and, thus, K may not be able to account for the entire fracture driving force. This is one of the reasons why the fracture toughness of a material measured in stress intensity factor may be influenced by the geometry of the test specimen and the loading condition [3-8].

3.9 IRWIN'S *K*-BASED FRACTURE CRITERION

From the continuum mechanics point of view, fracture is governed by the local stress and deformation conditions around the crack tip. It follows from the discussion in the last section that the near-tip stress field in the K-dominance zone can be represented by the inverse square-root singular stresses, which have universal functional forms in a local coordinate system centered at the crack tip. The geometries of cracked bodies and the loading conditions influence the crack tip singular field only through K (K_I, K_{II}, or K_{III} for different fracture modes), the stress intensity factor. Based on this fact, Irwin [3-1] proposed a fracture criterion, which states that crack growth occurs when the stress intensity factor reaches a critical value. Under Mode I conditions,

Irwin's criterion can be expressed as

$$K_I = K_c \tag{3.117}$$

where K_I is the applied stress intensity factor, which depends on the load level and the geometry of the cracked body, and K_c is the critical value of K_I at fracture, or fracture toughness.

Irwin's *K*-based fracture criterion differs from Griffith's free surface energy criterion in that the former focuses on the response of stresses near the crack tip, while the latter considers the global energy balance during crack growth. It will be shown in later chapters that these two criteria are equivalent only in elastic media.

It is apparent that the criterion Eq. (3.117) is established based on the assumption of linear elasticity with which the inverse square root singular stress field exists and the stress intensity factor is well defined. In other words, the complex fracture processes and the nonlinear deformations occurring around the crack tip are ignored. The validity of the criterion thus requires that the fracture process and nonlinear deformation zones are sufficiently small so that they are well contained inside the *K*-dominance zone around the crack tip, as shown in Figure 3.15. Thus, the value of K_c at the onset of unstable fracture taking place in the fracture process zone can be effectively employed to signify this event.

Theoretically, K_c in the criterion Eq. (3.117) should be a material constant and can be measured using standard specimens. However, K_c of a material may depend on the geometry of the test specimen and the loading condition as well. The variation of the *K*-dominance zone size is one of the causes for the variation of fracture toughness data [3-8]. Another main reason for the nonunique toughness is because the nonlinear deformation and fracture mode may depend on the geometry and loading condition. For instance, it is well known that K_c is highly sensitive to the thickness of the

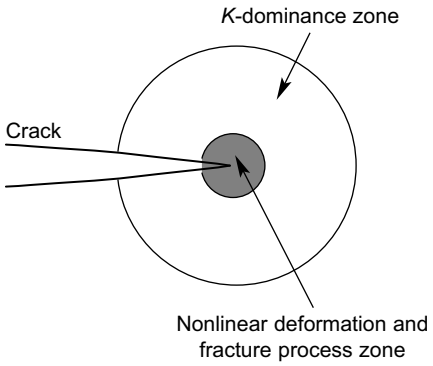

FIGURE 3.15

K-dominance zone around a crack tip.

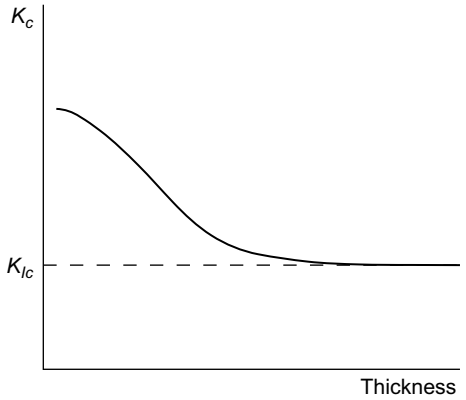

FIGURE 3.16

Thickness dependence of K_c, the critical stress intensity factor.

Table 3.1 Fracture Toughness for Typical Metals

Materials	K_{Ic} ($ksi\sqrt{in}$)	K_{Ic} ($MPa\sqrt{m}$)
Cast iron	30	33
Low carbon steel	70	77
Stainless steel	200	220
Aluminum alloy (2024-T3)	30	33
Aluminum alloy (7075-T6)	25	28
Titanium alloy (Ti-6Al-4V)	50	55
Nickel alloy (Inconel 600)	100	110

test specimen. This thickness dependence of K_c results from the plastic deformation around the crack tip. Thinner specimens permit greater plastic deformation and thus yield higher values of K_c.

In general, the measured critical stress intensity factor K_c for a metal becomes a constant (K_{Ic}) only when the thickness of the specimen exceeds a certain value and the stress field near the crack assumes the state of plane strain, as illustrated in Figure 3.16. The notation K_{Ic} is commonly used to denote the fracture toughness obtained under the plane strain condition. The standards of measuring K_{Ic} have been established by ASTM (American Society for Testing and Materials).

Table 3.1 lists values of plane strain fracture toughness values for common metals under room temperature conditions. It can be seen that the fracture toughness ranges from about $25\,MPa\sqrt{m}$ to $250\,MPa\sqrt{m}$ for these materials. The toughness for a specific material, however, may differ from the listed data. For engineering ceramics and polymers, the fracture toughness is usually less than $5\,MPa\sqrt{m}$.

In structural integrity design, fracture mechanics is typically used to predict the fracture strength of a structural member containing a given crack(s), or to predict an allowable length of a crack in a structural member subjected to a given load(s). For example, the stress intensity factor for a through-thickness axial crack in a thin-walled cylindrical pressure vessel is given by

$$K_I = \frac{pR}{t}\sqrt{\pi a}$$

where p is the internal pressure, a the half crack length, R the mid-surface radius and t ($\ll R$) the wall thickness of the vessel. If the plastic deformation is insignificant, the failure load (burst pressure) can be calculated by substituting this stress intensity factor in Eq. (3.117) for a given crack size $2a_0$ as follows:

$$p_{cr} = \frac{tK_{Ic}}{R\sqrt{\pi a_0}}$$

On the other hand, if the pressure level p_0 is specified according to the design requirement, the maximum allowable crack size can be calculated as follows:

$$a_{allow} = \frac{1}{\pi}\left(\frac{t}{R}\right)^2\left(\frac{K_{Ic}}{p_0}\right)^2$$

References

[3-1] G.R. Irwin, Analysis of stresses and strains near the end of a crack traversing a plate, J. Appl. Mech. 24 (1957) 361–364.

[3-2] N.I. Muskhelishvili, Some Basic Problems of the Mathematical Theory of Elasticity, P. Noordhoff Ltd., Groningen, Holland, 1953.

[3-3] H.M. Westergaard, Bearing pressures and cracks, J. Appl. Mech. 6 (1939) 49–53.

[3-4] G.C. Sih, On the Westergaard method of crack analysis, Int. J. Fract. Mech. 2 (1966) 628–631.

[3-5] M.L. Williams, Stress singularities resulting from various boundary conditions in angular corners of plates in extension, J. Appl. Mech. 19 (1952) 526–528.

[3-6] M.L. Williams, On the stress distribuion at the base of a stationay crack, J. Appl. Mech. 24 (1957) 109–114.

[3-7] S.G. Larsson, A.J. Carlsson, Influence of non-singular stress terms and specimen geometry on small-scale yielding at crack tips in elastic-plastic materials, J. Mech. Phys. Solids 21 (1973) 263–277.

[3-8] C.T. Sun, H. Qian, Brittle fracture beyond stress intensity factor, J. Mech. Mater. Struct. 4 (4) (2009) 743–753.

PROBLEMS

3.1 Given the Airy stress function as

$$\phi = Ay^2$$

derive the corresponding stress components and displacement components. Identify the rigid body terms in the displacement.

3.2 Use the relations between Z_I, Z_{II}, and ψ, χ to derive the stress function

$$\phi = \mathrm{Re}\{\widehat{\widehat{Z}}_I\} + yI_m\{\widehat{Z}_I\} - y\mathrm{Re}\{\widehat{Z}_{II}\} + Ay^2$$

3.3 Given $\phi = \mathrm{Re}\{\widehat{\widehat{Z}}_I\} + yI_m\{\widehat{Z}_I\}$, derive the stress and displacement components. Use only the definition of the stress function,

$$\sigma_{xx} = \frac{\partial^2\phi}{\partial y^2}, \quad \sigma_{yy} = \frac{\partial^2\phi}{\partial x^2}, \quad \sigma_{xy} = -\frac{\partial^2\phi}{\partial x \partial y}$$

the stress–strain relations, and the strain-displacement relations.

3.4 Find the stress function or Westergaard function that solves the problem of a crack of length $2a$ in an infinite plate. The crack surface is subjected to a uniform internal pressure p_0.

3.5 An infinite plate containing a crack of length $2a$ is subjected to a pair of compressive forces P as shown in Figure 3.8 (assume Q is zero in the figure). Show that the Westergaard function

$$Z_I = \frac{P}{\pi(z-b)}\sqrt{\frac{a^2-b^2}{z^2-a^2}}$$

is the solution and prove that the stress intensity factors at both crack tips are given by Eq. (3.76).

3.6 Consider a semi-infinite crack in an infinite plate opened by a pair of forces as shown in Figure 3.9. The corresponding Westergaard function is

$$Z_1 = \frac{P}{\pi(b+z)}\sqrt{\frac{b}{z}}$$

Prove that the stress intensity factor K_I is given by Eq. (3.81) and show that, for plane stress, the crack opening displacement is

$$\delta = \frac{4P}{\pi E}\ln\left|\frac{\sqrt{|x|}+\sqrt{b}}{\sqrt{|x|}-\sqrt{b}}\right|$$

3.7 An infinite plate containing a crack of length $2a$ is subjected to a uniform pressure p on the central portion of the crack faces from $x = -a_1$ to $x = a_1$ as shown in Figure 3.17. Determine the stress intensity factor using Eq. (3.79).

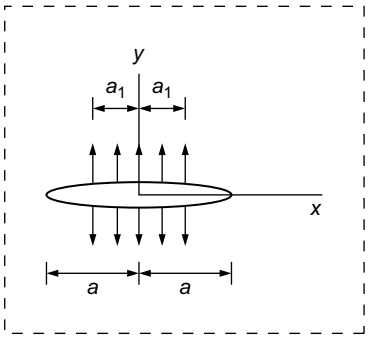

FIGURE 3.17

An infinite plate containing a crack of length $2a$ subjected to a uniform pressure p on the central portion of the crack faces.

3.8 An infinite plate containing a crack of length $2a$ is subjected to a bilinear pressure on the crack faces as shown in Figure 3.18. Determine the stress intensity factor using Eq. (3.79).

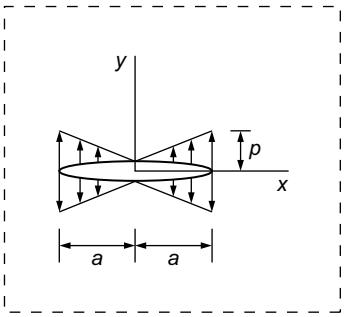

FIGURE 3.18

An infinite plate containing a crack of length $2a$ subjected to a bilinear pressure on the crack faces.

3.9 Consider an infinite plate containing an array of periodic cracks of length $2a$ subjected to biaxial tension σ_0 at infinity as shown in Figure 3.19. Show that

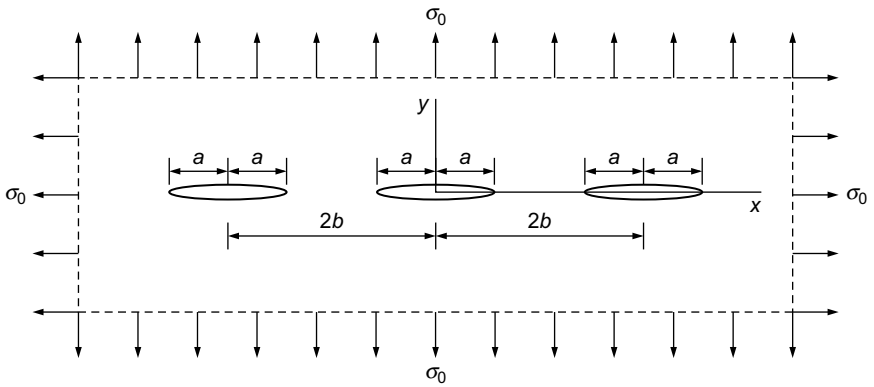

FIGURE 3.19

An infinite plate containing an array of periodic cracks of length $2a$ subjected to biaxial tension σ_0 at infinity.

the Westergaard function

$$Z_I = \sigma_0 \sin\left(\frac{\pi z}{2b}\right) \Big/ \sqrt{\sin^2\left(\frac{\pi z}{2b}\right) - \sin^2\left(\frac{\pi a}{2b}\right)}$$

is the solution and determine the stress intensity factor for the crack problem.

3.10 Consider an infinite plate with a central crack subjected to the remote tension along the y axis as shown in Figure 3.20. Find (a) σ_{yy} along the x axis (not the near crack tip solution), and (b) crack surface opening displacement u_y.

3.11 Consider Problem 3.4. Plot the degree of K-dominance along the crack line. Compare that with the case for which the plate is subjected to a remote tensile stress.

3.12 According to Williams' eigenfunction expansion for a Mode I crack, the opening stress ahead of the crack tip ($x > 0,\ y = 0$) is

$$\sigma_{yy} = \frac{K_I}{\sqrt{2\pi x}} + b_0 x^{1/2} + b_1 x^{3/2}$$

Find the values of b_0 for the two loading cases in Problem 3.11.

3.13 Check the accuracy of the formula Eq. (3.82) in conjunction with Eq. (3.83) by FEA or any numerical method of your choice.

3.14 Consider Problem 3.4. Replace the internal pressure with a pair of concentrated forces applied in opposite directions at the midpoint of the crack. Assume that these forces are applied to open the crack surfaces. Compare the

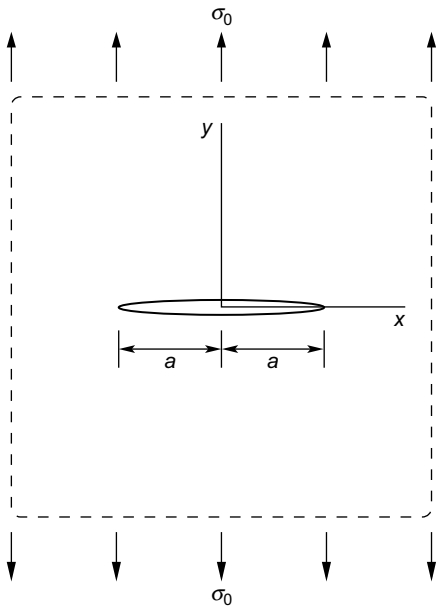

FIGURE 3.20

An infinite plate with a central crack subjected to the remote tension along the y axis.

K-dominance zone size of this loading with that of the remote stress loading case. If these two loading conditions are used to measure the fracture toughness of the material, which specimen would yield a higher toughness value in terms of K_I? Explain.